Zeitschrift: IABSE reports = Rapports AIPC = IVBH Berichte

Band: 67 (1993)

**Rubrik:** Selected papers

SELECTED PAPERS

Analytical Modelling for Fatigue Assessment of the Clifton Suspension Bridge
Modèle analytique d'évaluation de la fatigue du pont suspendu de Clifton
Analytisches Modell zum Ermüdungszustand der Clifton-Hängebrücke

M.S.G. CULLIMORE
Visiting Research Fellow
University of Bristol
Bristol, UK

Peter J. MASON
Director
Howard Humphreys & Partners
Dorking, UK

J. William SMITH
Senior Lecturer
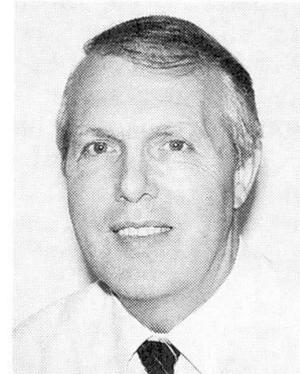University of Bristol
Bristol, UK

M. Stuart Cullimore, born 1920, graduated in civil engineering from Bristol University in 1940. Reader in Structural Engineering until 1985. Reserach latterly on fatigue of structural joints and bridge decks. Now Visiting Fellow at University of Bristol.
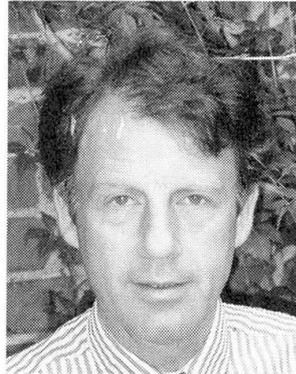
Peter Mason, born 1945, joined the Bridge Department of Howard Humphreys & Partners, consulting engineers, in 1967 on graduating from Imperial College, London. He is now a director of the company and is responsible for all the firm's structural engineering work.

William Smith, born 1941, graduated in Civil Engineering at the University of Edinburgh, Scotland. Obtained his PhD (vibration of bridges) at the University of Bristol where he now studies dynamic loading and fatigue of bridges.

SUMMARY

The Clifton Suspension bridge is an iron eye-bar chain suspension bridge of 214 m span. Despite its age (128 years) it is a vital link in the traffic system of Bristol, carrying nearly 4 million vehicles per year. An extensive structural assessment of the bridge has been carried out. This has required global analytical modelling, load testing, strain monitoring under traffic, and fatigue appraisal of the major components.

RÉSUMÉ

D'une portée de 214 m, le pont suspendu de Clifton est supporté par des chaînes formées de barres à oeil. Malgré son âge de 128 ans et avec près de 4 millions de véhicules par année, il constitue un élément de liaison essentiel pour le trafic routier de Bristol. Au cours de l'évaluation de la sécurité à la ruine à l'aide d'un modèle analytique appliqué à la structure complète, il a été procédé à des essais de charge et à des mesures de déformation sous charge mobile, ainsi qu'à la vérification de la fatigue de tous les éléments porteurs principaux.

ZUSAMMENFASSUNG

Die Clifton-Hängebrücke mit 214 m Spannweite wird von Ketten aus eisernen Augenstäben getragen. Trotz ihres Alters von 128 Jahren stellt sie mit fast 4 Mio. Fahrzeugen pro Jahr eine Hauptverbindung im Verkehrsnetz von Bristol dar. Bei der notwendigen Tragsicherheitsüberprüfung anhand eines analytischen Modells des gesamten Tragwerks wurden Probebelastungen, Dehnugsmessungen unter Verkehr und Ermüdungsnachweise aller Hauptkomponenten durchgeführt.

1. INTRODUCTION

The Clifton Suspension Bridge was designed originally by the eminent Victorian engineer Isambard Kingdom Brunel. The bridge was completed in 1864, after his death, with a number of important modifications to his design [1]. The spectacular setting of the bridge spanning the Avon Gorge makes it an important tourist attraction and focus of civic pride (Fig 1). But it is also an important link in the traffic system of Bristol carrying nearly 4 million vehicles per year, although there is a gross weight limit of 40 kN.
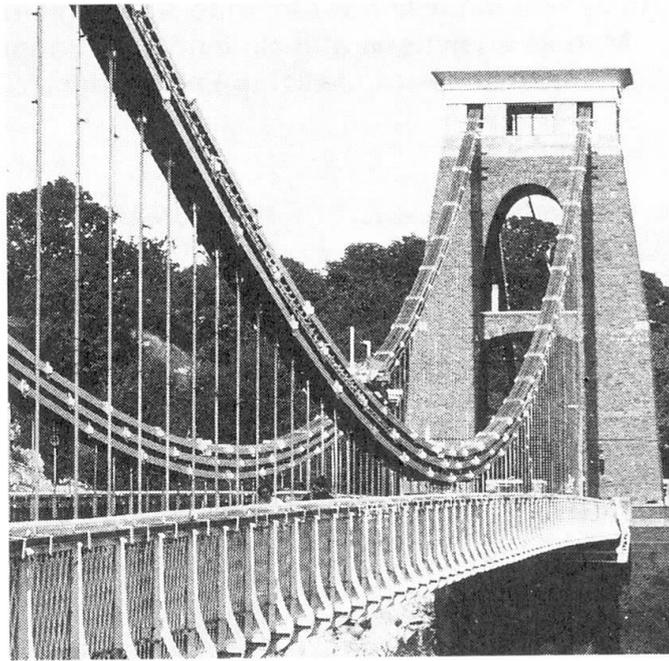
Fig 1 Clifton Suspension Bridge

Structurally the bridge is a wrought iron eye-bar suspension chain with a suspended structure carrying an asphalt surfaced timber deck (Fig 2). There are three chains on each side of the roadway, arranged one above the other as shown in Fig 1. They are made up of 175mm x 25mm wrought iron bars with special eye joints forged to each end. Each link is made up of ten or eleven bars arranged side by side, interleaved with the bars of the next link, and connected with a pin through the eye joint. Successive suspender rods, at intervals of 2.44m (8 feet) are attached to each of the three chains in turn, (see Fig 1), so that the eye-bars are approximately 24 feet in length depending on the local slope of the chain. The wrought iron suspended structure (Fig 2) consists of longitudinal riveted plate girders, under each set of chains, lattice cross-girders and longitudinal lattice parapet girders. The roadway deck is timber with mastic asphalt surfacing.

Fig 2 The suspended structure

A number of studies of the structural capacity of the bridge have been undertaken this century, some of them resulting in remedial or strengthening works [1,2]. The collapse of the Point Pleasant Bridge over the Ohio river in 1967, resulting from corrosion-fatigue in an eye bar, prompted an extensive fatigue appraisal of the Clifton Bridge [3]. It was concluded that there was an adequate margin of safety against fatigue failure at that time. However, traffic loading was steadily increasing and ther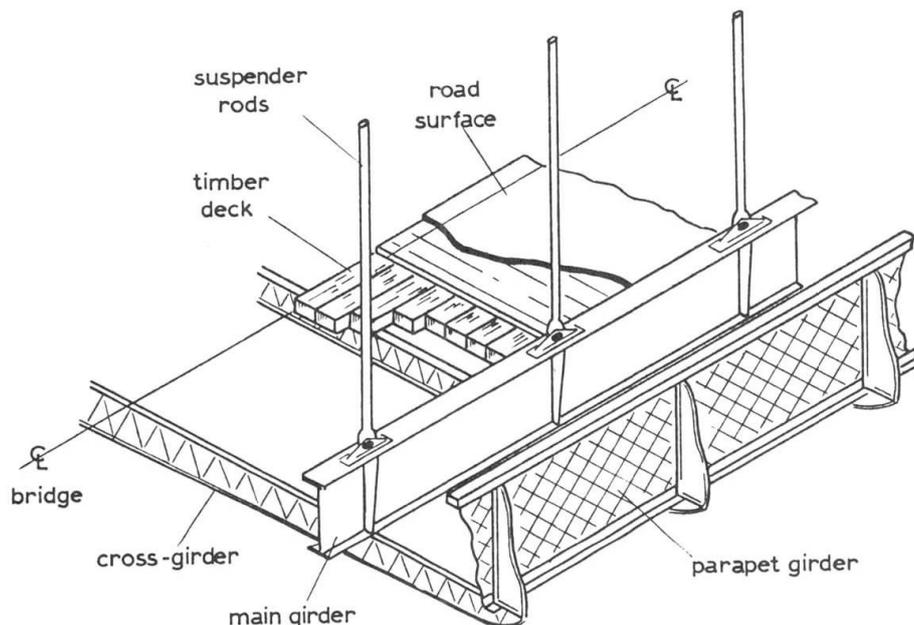e was concern over progressive deterioration of the riveted joints of the parapet girder and other signs of wear or damage. It was decided that a global analysis of the structure should be carried out, using modern analytical methods, so that the effects of a range of load cases could be studied.
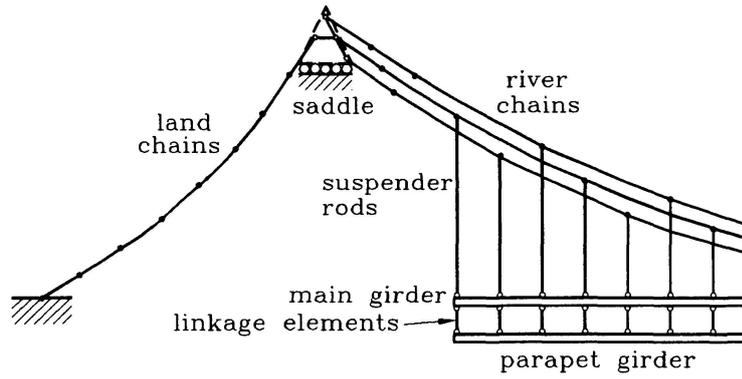
2. FINITE ELEMENT MODEL

2.1 Modelling assumptions and analytical procedure

Suspension bridge behaviour under load is geometrically non-linear. This is because the cable or chain adapts its shape when a concentrated load is applied at a particular point on the structure. In most suspension bridges, as at Clifton, the longitudinal girder provides some stiffening and effectively distributes these deformations over part of the structure. For this reason it was decided to use a finite element program which had geometrically non-linear solution capabilities.

The finite element model was designed to represent the effects of vertical loading on the structure. For this purpose a two-dimensional model was considered to be adequate. Dead load and traffic load in both lanes is symmetrical about the longitudinal axis of the bridge and therefore only one half of the bridge needed to be modelled, i.e. one set of three chains supporting the main girder and parapet girder. Eccentric traffic loads, in the form of single vehicles or traffic in one lane only, were dealt with by means of a separate torsional analysis.

A schematic diagram of the node and element geometry is shown in Fig 3a. From the left anchorage to the tower the three chains were represented by a single chain of beam elements. The final link was connected by a pin joint to the saddle elements. The saddle nodes were all effectively constrained to move horizontally as a single unit, simulating the roller bearing that exists at the top of each tower. The three chains of the main span were represented by beam elements of the same length as each eye bar link. Thus the correct sequence of connection to the suspender rods could be modelled as shown. Each link of ten, eleven or twelve bars, was modelled by a single element of equivalent area. It has been observed that the chain links behave as if they are rigidly connected to each other over the main part of the span. The pins work freely only at the tower saddles. The main girder was modelled by beam elements pin connected to the vertical rods as shown. There is no vertical or horizontal restraint to movement of the main girders of the bridge. However, in order to avoid computational instability, a soft horizontal spring restraint was connected to the middle node of the deck.

The behaviour of the cross girders and parapet girder were modelled by suspending longitudinal beam elements from the main girder elements by means of vertical linkages. The stiffness of the linkage elements was determined from the stiffness of the cross girder in shear between points of connection of the main and parapet girders as shown in Fig 3b. In order to avoid the problem of horizontal instability it was sufficient to introduce horizontal coupling between main and parapet girders at mid-span.

(a) Schematic diagram of node and element geometry

Stiffness of linkage element, k = P/Δ
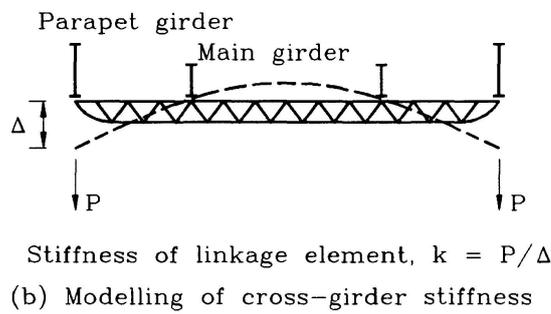
(b) Modelling of cross-girder stiffness

Fig 3   Finite Element Model

2.2 Analysis of eccentric loading

It was mentioned earlier that eccentric loads, such as single vehicles or traffic in one lane only, could be dealt with by introducing a torsional component. This is illustrated in Fig 4 where it can be seen that the loading can be resolved into symmetric and torsional components at the line of the chains. If the cross girder is rigid, then because of its rotation about the centre line, it forces the parapet girder to deflect more than the main girder in the torsional case. Hence the effective stiffness of the parapet girder, if it is transposed to the same plane as the main girder and the chains, becomes:

$$I_{effPa} = I_p(B/b)^2 \hspace{4cm} (1)$$
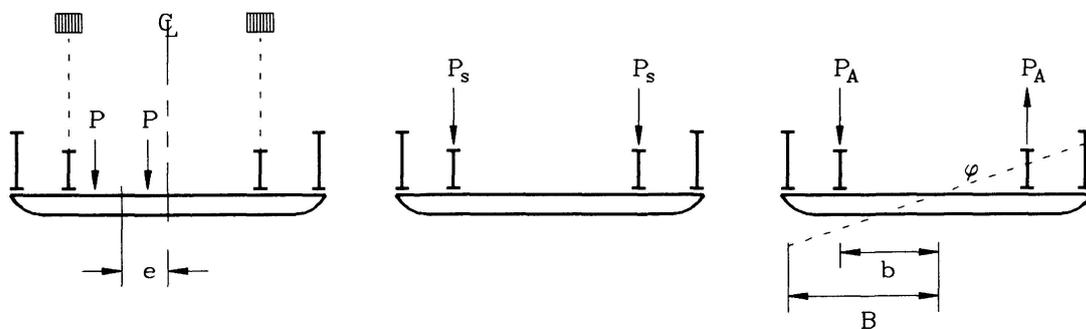
Symmetric component P_S = P
Torsional component P_A = P.e/b

Fig 4   Analysis of eccentric loading

In this way it would be possible to analyse the problem as two separate load
cases and add the results, provided that it could be assumed that deflection
of the chains was linear with changes in live load applied at a point.   In
practice it was possible to combine the symmetric and torsional components
into a single eccentric load case.   This was done by evaluating the effective
stiffness of the parapet girder when transposed to the line of the chains with
both symmetric and torsional component loads present.   The formula is as
follows:

$$I_{effp} = I_p \left[\frac{B^2}{B^2 + fb^2} \right](1 + f) \; ; \quad \text{where} \quad f = P_a/P_s \qquad (2)$$

Further refinements were included which took account of cross girder
flexibility in the torsional case, but are outside the scope of this paper.

2.3 Load tests and comparison with analytical model

In order to confirm the analytical model, loading tests were carried out on
the bridge at night.   The weight limit on the bridge is 40 kN.   This
represents vehicles such as ambulances, loaded vans and pick-up trucks.   Two
loading cases were identified as follows:

(a) Dual vehicle symmetric loading
The maximum concentrated load occurs when two 40 kN vehicles, travelling in
opposite directions, pass each other on the span.   Assuming a load
distribution of 15 kN at front axles and 25 kN at rear axles the load case is
as shown in Fig 5.   Although the front axles are in opposite lanes of the
carriageway, and would produce an anti-symmetric torsional component of
loading, it was assumed that this would be a small localised effect and that
the load could be treated as symmetric as shown.

b = 3.66 m
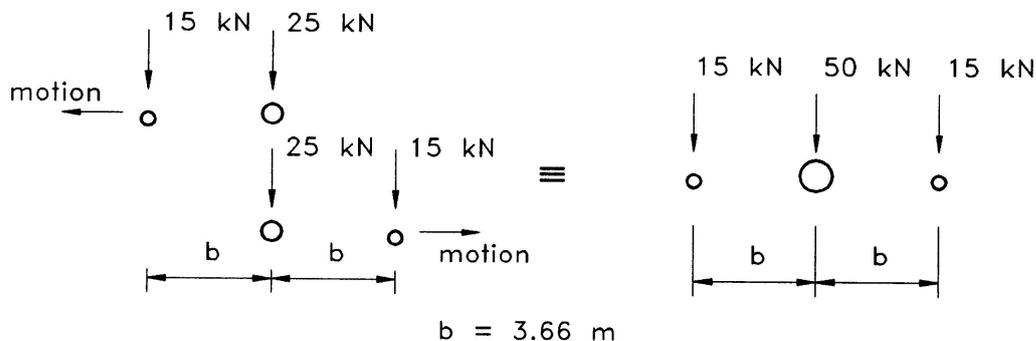
Fig 5   Dual vehicle load case (symmetric)

(b) Single vehicle eccentric loading
The bridge is torsionally flexible and therefore it was considered important
to study the effects of a single 40 kN vehicle travelling in one lane of the
carriageway, thereby applying an eccentric loading to the structure.   The
eccentricity of the vehicle in the analysis was taken as 1.0 m from the centre
line of the carriageway.

For the loading tests on the bridge, two pick-up trucks were hired and loaded
with boxes of nails to provide the appropriate distribution.   Strain gauges
were fixed to the top and bottom flanges of one parapet girder and both main
girders at 1/4 span.   The signals were logged by a computer data acquisition
system while the vehicles were crossing the span in the loading configurations
described above.

The results of a typical analysis are shown in Fig 6 and the results of a single vehicle load test run are shown in Fig 7. Similarity in the shapes of the curves is evident. The test run results are effectively influence lines for strain at 1/4 span when the vehicle passes over the span. The analysis represents the distribution of deflection and bending moments when the vehicle is stationary at the 1/4 point. But since the wheel base of the vehicle is very short compared with the span, and there is evidence of linearity under live loads, it may be considered that the analysis results approximate to influence lines. It may also be noted that the bending in the main girder is sharper than that of the parapet girder directly under the load. This is because flexibility of the cross girder results in transfer of bending from the main to parapet girder to be distributed longitudinally to some extent. A further point to note about the results is that the parapet girder bending moment is of the same order as that of the main girder. It is not known if this structural action of the parapet girder was taken into account in the original design.

Main Girder Bending Moment
Max BM = 64.0 kNm

Parapet Girder Bending Moment
Max BM = 70.6 kNm
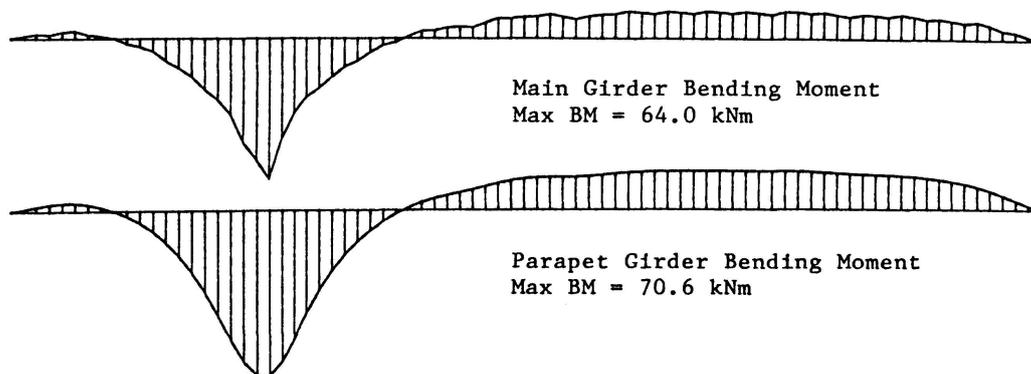
Fig 6   Finite element analysis of eccentric 40 kN load at 1/4 span

(a) Main Girder (bottom)

(b) Parapet Girder (bottom)
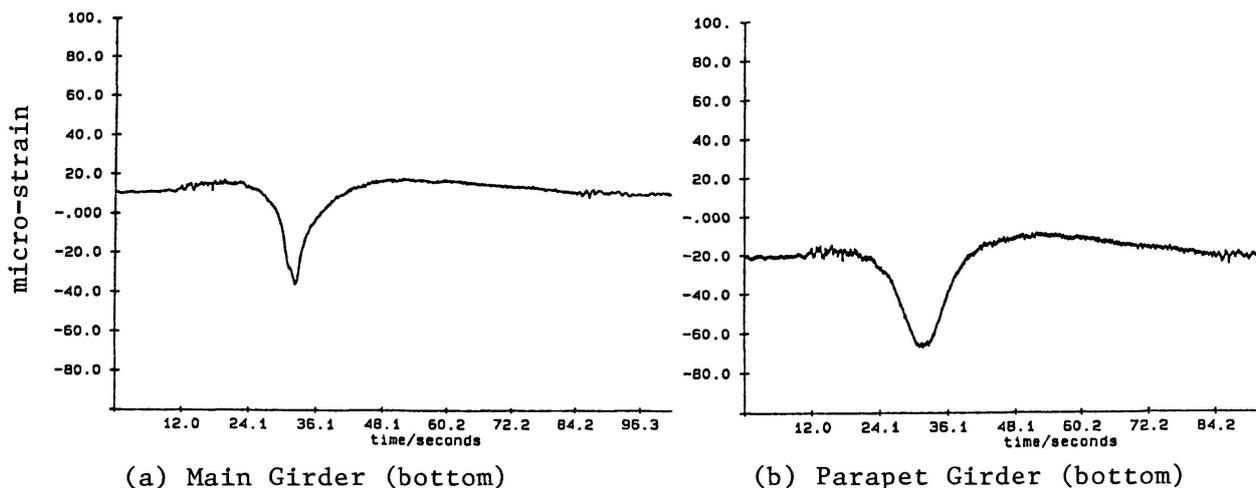
Fig 7   Strains at 1/4 span under action of 40 kN vehicle eccentric load

In order to obtain quantitative comparison between the experimental results and the analysis it was necessary to convert the observed strains at top and bottom of the girders to equivalent bending moments. This was done using the measured sectional properties of the girders and a value of E for wrought iron of 192 GN/m^2. The results are compared in Table 1 below.

Table 1 Bending Moments at 1/4 span in kNm (analysis in parentheses)

LOAD	POSITION	MAIN GIRDER		PARAPET GIRDER		TOTAL MOMENT	
8 ton	1/2 span	18.2	(19.7)	13.1	(24.6)	38.4	(44.3)
symm.	3/8 "	3.3	(4.0)	5.3	(1.8)	11.6	(5.8)
	1/4 "	-89.1	(-111.7)	-64.1	(-86.3)	-170.6	(-198.0)
	1/8 "	-2.1	(-8.5)	-7.0	(-10.6)	-18.8	(-19.1)
4 ton ecc.	1/4 "	-56.4	(-64.0)	-43.7	(-70.6)	-111.2	(-134.6)

In Table 1 the experimental moments were evaluated from the strain gauge data so as to provide a comparison with the analysis. The analytical results are generally greater than the experimental results. This is probably a result of the influence of the deck which acts like an additional flange to the main girder. This was difficult to include in the analytical model although some allowance was made by modifying the girder section properties to simulate the shift of the neutral axis.

The 'Total Moment' in Table 1 is the sum of the girder moments in the case of the analysis. However, the longitudinal forces introduced by the presence of the deck could be evaluated from the strain gauge data together with the girder moments. Hence, the 'Total Moment' of the experimental results is always greater than the direct sum of the girder moments.

3. CONTINUOUS MONITORING OF GIRDER STRAINS UNDER NORMAL TRAFFIC

3.1 Installation and use of "Stress Analyser"
The same strain gauge locations, as used in the vehicle loading tests, were monitored continuously under normal traffic for several one week periods. The equipment for doing this, called a "Stress Analyser" [4], was capable of amplifying the signal from the gauges, detecting peaks and troughs of the fluctuating signal, and performing a "rainflow" count in real time. "Rainflow" counting is an accepted method for interpreting a varying amplitude signal in terms of an equivalent number of simple cycles of different amplitudes. The fatigue damaging potential of the signal may then be assessed by summing the fatigue damage contributions of all the simple cycles.

The data are provided in the form of numbers of cycles of different strain ranges. The mean strain was not recorded because, although it has an effect it is generally accepted that, for materials such as wrought iron with many defects, strain range is the dominant factor affecting fatigue life.

3.2 Prediction of strain range cycle count and comparison with observations
The results of the global analysis were used to make a prediction of the strain range cycle count under normal traffic. This was achieved by looking at the output from the analysis of the bridge under a 40 kN eccentric load as shown in Fig 6. It has already been said that this figure approximates to an influence line and therefore the range of bending moment at the 1/4 span when a 40 kN vehicle crosses the bridge may be deduced from the maximum and minimum of this figure. It was further assumed that the bending moments at this point were linear with load within the range of live loading. Hence, it was possible to evaluate strain ranges occurring under the passage of a range of vehicle weights as they cross the bridge.

A classification count was carried out on the bridge, grouping weekday traffic into seven weight classes. Cars were relatively easy to classify according to weight, but estimates had to be made for larger vehicles such as pick-up

trucks, vans and ambulances. A count was also made of the number of times vehicles travelling in opposite directions were applying load to a particular cross girder simultaneously. The count is set out in Table 2 below.

Table 2   Number of loadings of a cross girder by vehicles of different weight

Vehicle weight	8	10	14	20	25	30	40	(kN)
Left lane	264	633	252	26	22	11	2	
Right lane	343	819	243	41	22	11	3	
Both	21	184	56	10	1			

The weights were converted into strains at the top of the main girder and a table of the number of loading cycles within strain range bands was compiled. Data on the number of vehicle crossings was available from the toll records and amounted to 72,000 vehicles per week during the period of the study. The number of cycles for the short count (four hours in total) was then factored up to give the number of cycles that would occur at the same rate during one week of normal traffic. The predicted cycle count was compared with the data obtained using the "Stress Analyser" and is shown in Table 3.

Table 3   Strain range cycle count: Predicted v. Stress Analyser

Strain Range ($\times 10^{-6}$)	Number of Loading Cycles		
	Predicted		Stress Analyser (avg
	Short count	Seven days	of 3 seven day periods)
0 - 10	343	8,332	124,022
10 - 20	1,326	32,210	20,713
20 - 30	695	16,882	12,403
30 - 40	469	11,393	6,989
40 - 50	82	1,992	3,328
50 - 60	25	607	1,356
60 - 70	21	510	519
70 - 80	1	24	174
80 - 90	2	48	59
90 - 100			18
100 - 110			7
110 - 120			3
120 - 130			1

Considering the difficulties of assessing the loads from the visual classification count the correlation is remarkably good. The large number of cycles occurring in the smallest strain range may be the result of small vibrations and electronic noise. A further comparison can be made by evaluating the fatigue damage done by each loading cycle. This can be achieved by assuming a power law for fatigue life with an index of 3, together with Miner's law of cumulative damage. It is then possible to calculate the equivalent strain range per vehicle, if applied repetitively, that would yield the same fatigue damage as the actual variable loads. This quantity (ESRV) is given by

$$\text{ESRV} = (n_i S_i^m / 72,000)^{1/m} \qquad\qquad (3)$$

where n_i is the number of cycles of strain range S_i and m is the index of the power law. m=3 is a reliable mean value for fatigue of wrought iron.

Using the data in Table 3 the following comparison may be made:

ESRV predicted = 26.4 x 10^{-6}
ESRV experiment = 26.8 x 10^{-6}

This result confirms that the method of prediction provides a very accurate measure of fatigue damage.

4. FATIGUE ASSESSMENT OF MAJOR COMPONENTS

4.1 Saddle link
Rotation of the chain links attached to the saddle bearings at the tops of the towers were found to produce significant variations in principal stress while vehicles crossed the bridge. In an earlier study this was found to be the most significant fatigue loading on the bridge [3]. The results of the load tests carried out on the bridge at that time were found to compare favourably with the global analysis. Hence the conclusion of the earlier assessment, that there was sufficient factor of safety against fatigue or fracture, was confirmed.

4.2 Main girders
The strains observed in the main girder under normal traffic (Table 3) were converted to stress cycles. These were compared with S-N curves for riveted girders [5,6]. Assuming traffic totalling 4 million vehicles per year the fatigue life of the main girder was calculated to be 468 years.

4.3 Parapet girders
For fatigue loading the critical location is the spliced joint in the top flange of the parapet girder. Strains were obtained using the same procedure as for the main girders and were converted to stress ranges. The joints have been progressively deteriorating in recent years and a new friction grip bolted assembly has been designed as a replacement. Using the current UK code for fatigue assessment, the life of the joint was estimated to be 197 years.

REFERENCES

1. MITCHELL-BAKER D and CULLIMORE M S G., Operation and maintenance of the Clifton Suspension Bridge. Proc Inst Civil Engrs, Part 1, n 84, 291-308, April 1988.

2. FLINT A R and PUGSLEY A G., Some experiments on Clifton Suspension Bridge. Correlation between calculated and observed stresses and displacements in structures. Inst Civil Engrs, Preliminary vol, 124-134, London 1955.

3. CULLIMORE M S G and MASON P J., Fatigue and fracture investigation carried out on the Clifton Suspension Bridge. Proc Inst Civil Engrs, Part 1, n 84, 309-329, April 1988.

4. WASTLING M A and SMITH J W., An instrument for detecting arbitrary peaks and troughs of a fluctuating stress signal. Strain, Brit Soc Strain Measurement, 127-131, August 1987.

5. BRUHWILER E, SMITH I F C and HIRT M A., Fatigue and fracture of riveted bridge members. J.Struct.Engng., ASCE, v116, n1, 198-214, 1990.

6. FISHER J W, YEN B T and WANG D., Fatigue strength of riveted bridge members. J.Struct.Engng., ASCE, v116, n11, 2968-2981, 1990.

Long-term Prediction of Behaviour of Cable-Stayed Bridges
Prédiction du comportement à long terme de ponts à haubans
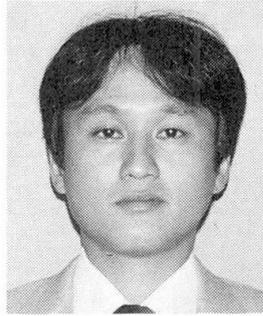## Voraussage des langfristigen Verhaltens von Schrägseilbrücken

Eiichi WATANABE
Professor
Kyoto University
Kyoto, Japan
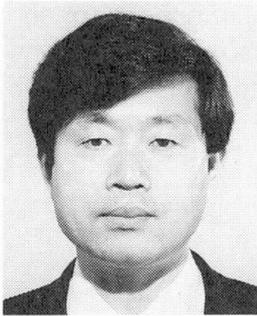
Eiichi Watanabe, born 1942, B.S., M.S. & Dr. Eng. from Kyoto University, M.S. & Ph.D. from Iowa State University, USA.

Masahiro KAMEI
Chief Engineer
Osaka Municipial Office
Osaka, Japan

Born 1950, B.S., M.S. from Osaka City University.

Luiza H. ICHINOSE
Bridge Engineer
Harumoto Iron Works, Co. Ltd
Osaka, Japan

Born 1960, B.S. from Federal University Rio de Janeiro, Br., M.S. from Kyoto University.

Osamu NAKADE
Bridge Engineer
Misubishi Heavy Ind. Ltd
Hiroshima, Japan

Osuma Nakade, born 1963, B.S., M.S. from Osaka University.

Yasuhiro ISHIHARA
Bridge Engineer
Katayama Strutech Corp.
Osaka, Japan

Yasuhiro Ishihara, born 1954, B.S. from Kobe University.

SUMMARY

Presented herein is a method to predict the long-term change of cable forces and slip of cables out of sockets in cable-stayed bridges. Employed are full-scale long-term tension tests of cables to determine the visco-elastic constants of the cables and the sockets. Based on the experimental results, the analytical prediction of bridges were made through the finite element visco-elastic analysis together with the Laplace transform and the results were compared to the site measurement values.

RÉSUMÉ

Cet article présente une méthode pour évaluer le comportement à long terme des contraintes des câbles d'un pont à haubans, ainsi que le comportement au glissement de ses ancrages. Des essais du câble en vraie grandeur on été effectués afin de déterminer les propriétés visco-élastiques des câbles et des ancrages. La méthode des éléments finis combinée avec la transformation de Laplace est appliquée à l'analyse et les résultats analytiques sont comparés avec les mesures effectuées sur le chantier.

ZUSAMMENFASSUNG

Es wird eine Methode vorgestellt, mit der langfristige Veränderungen in den Seilkräften, einschliesslich Schlupf in den Verankerungen, vorausberechnet werden können. Dazu waren im Massstab 1:1 Versuche zur Bestimmung der viskoelastischen Eigenschaften von Seilen und Ankerköpfen nötig. Mit diesen Daten wurden Finite-Element-Berechnungen für Brücken unter Verwendung der Laplace-Transformation durchgeführt und die Ergebnisse mit In-Situ-Messungen verglichen.

1. INTRODUCTION

Presented herein is a method to predict the long-term change in the cable forces and cables slip-out from their sockets in cable-stayed bridges. Based on long-term tension tests on full-scale cables of 5m length, a very simple analytical model is proposed and an effort is made to determine the visco-elastic constants of the cables and sockets, taking into account the scale effect of the length of the cables, by extrapolating the results of the measurements carried out in cables with limited length to actual cables with arbitrary length. In addition, visco-elastic F.E.M. analysis using the experimental results was carried out to predict the long-term behavior of several existing bridges and these results were compared to the measured values at the site.

Due to the fact that the erection of bridges is usually completed within a period of one year or one year and a half at the site, the visco-elastic constants of the cables and sockets were determined emphasizing first, the initial relatively short period of the erection stages and, secondly, focusing on the control of the cable forces for the much longer period of service life.

2. LONG-TERM TEST OF PROTOTYPE CABLES

2.1 Experimental Method

When investigating the time-dependent behavior of materials, there are two types of tests, namely, creep and relaxation tests. The former being carried out under constant loading with increasing deformation, and the latter under constant deformation with decreasing stress. The type of test carried out in the present study is a combination of both types [1].

The measurement system is presented in Fig.1, where the load is measured by a load cell and the relative displacements between the cable and the steel frame, by displacement transducers. To investigate the visco-elastic characteristics of the cables due to the difference in cable strength, two types of cables (Specimen types 1 and 2) were tested. In addition, four different combinations of cables and sockets (Specimen types 3 to 6) were tested, in a total of 6 specimens. Table 1 shows the specimen dimensions and characteristics.
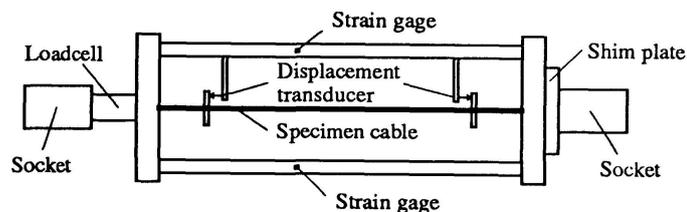
Fig.1 Measurement System

Table 1 Dimensions and Characteristics of the Test Specimen

Specimen Name	Type 1	Type 2	Type 3	Type 4	Type 5	Type 6
Cable Length (m)	5.9	5.9	5.4	5.4	5.4	5.4
Diameter of Wire (mm)	5.0	5.1	7.0	7.0	7.0	7.0
Number of Wires	127	127	19	19	19	19
Cable Type	PWS	PWS	PWS	PWS slightly twisted	PWS	PWS slightly twisted
Anchorage Length(cm)	44.0	44.0	16.3	16.3	30.7	30.7
Anchorage Type	Zinc-poured	Zinc-poured	HiAm	HiAm	Zinc-poured (Incl. 2% Cu)	Zinc-poured (Incl. 2% Cu)
Cross Sectional Area (cm²)	24.94	25.94	7.31	7.31	7.31	7.31
Breaking Force (kN)	4400	3910	1137	1137	1137	1137
Initial Cable Force (kN)	1400	1310	380	377	368	371

2.2 Test Results

Fig.2 shows the time variation of the tensile force in the cables. As it can be observed, the forces in specimen types 3 and 4 tend to stabilize in a relatively short time (about 20 days), whereas in the other cables, continue to decrease even after one year's measurement.

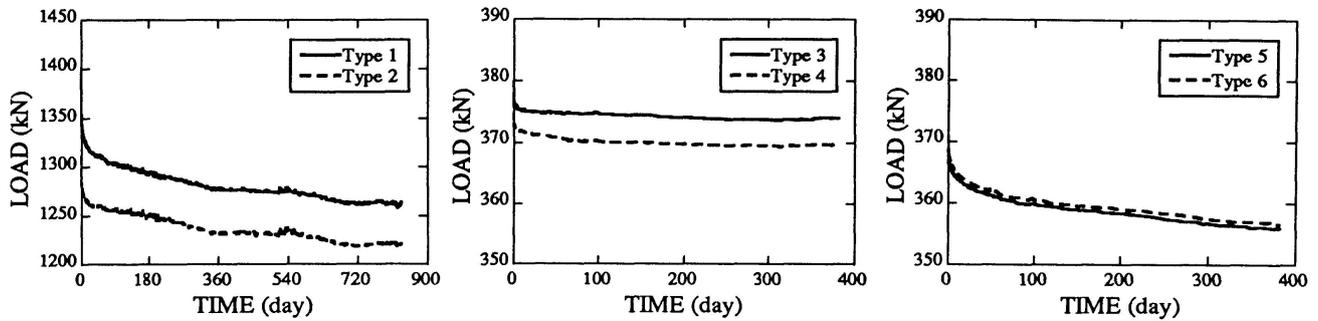Fig.2 Time Variation of Cable Tensile Force

Although the tested cables and sockets were the same as the ones used in actual bridges, the cable length of the specimens differed from the actual cables, thus, it was decided herein to consider the cables and sockets separately. Fig. 3 illustrates the time-dependent strain of each cable type and Fig.4, the slip-out behavior of the different types of sockets.
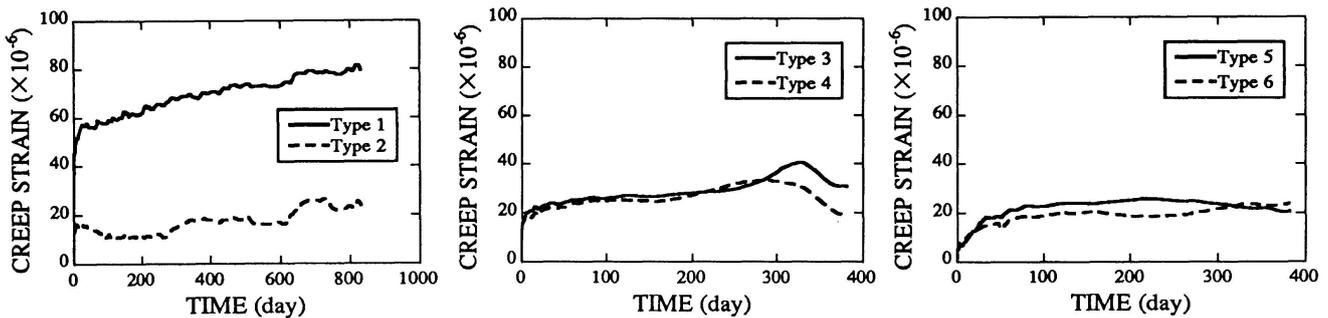
Fig.3 Time-dependent Behavior of Cables
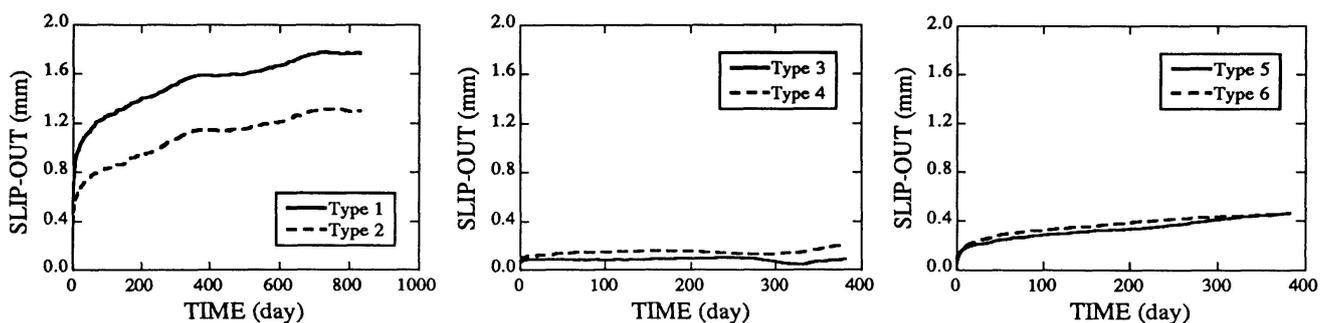
Fig.4 Time-dependent Behavior of Sockets

Specimen types 1 and 2 presented large values for the amount of slip-out from the sockets, compared to the values of cable creep. Specimen type 3 and 4, 5 and 6 have respectively the same sockets. In the formers, the forces, as well as the amount of slip-out stabilized in relatively short time (20 days); whereas in the latters, the amount of slip-out continued to increase.

Cable material of the specimen types 3 and 5, 4 and 6, being respectively the same, presented similar values for the final creep. However, time variation between cables of the same type were different, suggesting the influence of their sockets.

3. MODEL TO EVALUATE TIME-DEPENDENT CONSTANTS

3.1 Mechanical Model

Due to its simplicity, the analytical model adopted is the three-element model shown in Fig.5 [2]. The total strain of the model ε, can be expressed as the sum of the elastic (ε_e) and viscous (ε_v) strain:

$$\varepsilon = \varepsilon_e + \varepsilon_v \qquad (1)$$

For the total stress σ, the strain-stress relationship can be expressed as follows:

$$\sigma = \sigma_e = E_1 \varepsilon_e \qquad (2)$$

$$\sigma = \sigma_v = E_2 \varepsilon_v + \eta \dot{\varepsilon}_v \qquad (3)$$

Fig.5 Three-element Visco-elastic Model

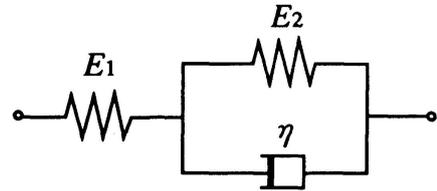where E_1, E_2 are the elastic coefficients and η the viscosity coefficient of the three-element model. Differentiating Eq.1 and Eq.2 in relation to time t and introducing them in Eq.3, it yields the following equation, after some arrangement.

$$\dot{\sigma} + \frac{E_1 + E_2}{\eta} \sigma = E_1 (\dot{\varepsilon} + \frac{E_2}{\eta} \varepsilon) \qquad (4)$$

3.2 Evaluation of Time-dependency

The visco-elastic constants of the model were evaluated according to the three different methods described bellow.

3.2.1 Method 1

Focusing on the viscous part of the model in Fig.5 (Eq.3) the following approach curve for the strain due to the viscosity was assumed.

$$\varepsilon_v = \bar{\varepsilon}_v (1 - e^{-\lambda t}) \qquad (5)$$

The coefficient λ can be obtained through the least square method. The results of the evaluation for one of the cables is shown in Fig.6, with the corresponding slip-out from the sockets shown in Fig.7 and the viscosity constants thus evaluated are presented in Table 2.

This method is effective for cables in which the phenomena of creep and slip-out from the sockets stabilize in a short time, however, in cases in which the time dependent curves are not steep and long-term variation is observed, the curves tend to diverge from the predicted values.
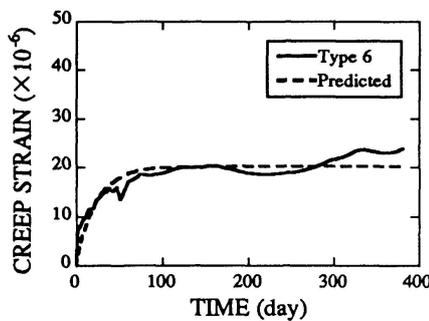
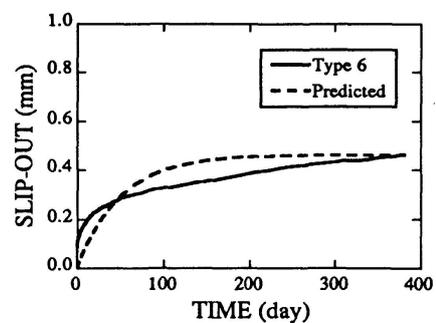**Fig.6** Predicted Time-dependent Behavior of Cables (Method 1)

Fig.7 Predicted Time-dependent Behavior of Sockets (Method 1)

Table 2 Evaluated Visco-elastic Constants (Method 1)

Specimen	Cable				Socket			
	$1/\lambda$ (day)	E_1 (GPa)	E_2 (GPa)	η (year GPa)	$1/\lambda$ (day)	K_1 (MN/m)	K_2 (MN/m)	η (year MN/m)
Type 1	2.97	217	6272	51.0	80.0	381	704	154
Type 2	0.26	196	30184	21.5	113.6	543	948	295
Type 3	1.168	202	19306	61.8	0.153	210	4192	1.76
Type 4	1.043	201	20690	59.1	1.188	228	2454	7.99
Type 5	25.5	191	20482	1428.4	75.0	785	769	158
Type 6	23.0	198	24304	1533.1	50.3	582	769	106

3.2.2 Method 2

The prediction of the time dependent behavior of bridges during their construction stages requires more accurate values for the initial steep part of the time variation curves. Thus, in the second method, the equations used in Method 1 were applied to a relatively short time interval corresponding to the average interval of time between the prestress of one of the cables and the prestress of the cable of the succeeding stage. This method converges for the initial part of the time variation curves and leads to reliable values for the initial 40 days. Fig.8 shows one of the curves evaluated by this method with the respective experimental curve. Table 3 presents the visco-elastic constants evaluated for specimen types 1,2,5 and 6.

Table 3 Evaluated Visco-elastic Constants for Sockets (Method 2)

Specimen	$1/\lambda$ (day)	K_1 (MN/m)	K_2 (MN/m)	η (year MN/m)
Type 1	0.921	381	1491	3.76
Type 2	1.043	543	2154	6.16
Type 5	2.48	785	2030	13.8
Type 6	1.319	582	1910	6.90
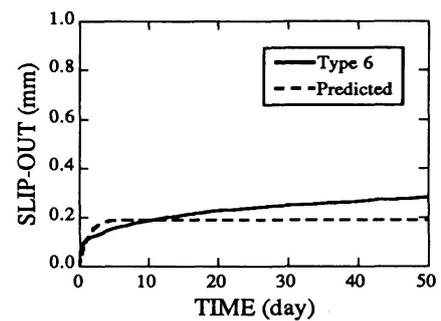
Fig.8 Predicted Time-dependent Behavior of Sockets (Method 2)

3.2.3 Method 3

For the maintenance of the bridge during its service life, a long-term prediction is necessary and the strain variation for the time period succeeding the one considered in Method 2, shall be assumed as it follows.

$$\varepsilon_v = \bar{\varepsilon}_v(1 - \alpha e^{-\lambda t}), \quad \text{where} \quad \lambda = E_2 / \eta \tag{6}$$

Considering $\bar{\varepsilon}_v$ as a determined parameter, α and λ can be determined by the least square method. Fig.9 illustrates the results of the analysis for one of the specimens and Table 4 shows the evaluated visco-elastic constants for specimen types 1, 2, 5 and 6.

Table 4 Evaluated Visco-elastic Constants for Sockets (Method 3)

Specimen	α	$1/\lambda$ (day)	K_1 (MN/m)	K_2 (MN/m)	η (year MN/m)
Type 1	0.450	351	344	684	658
Type 2	0.541	413	491	866	980
Type 5	0.748	607	505	479	797
Type 6	0.588	178	406	731	356
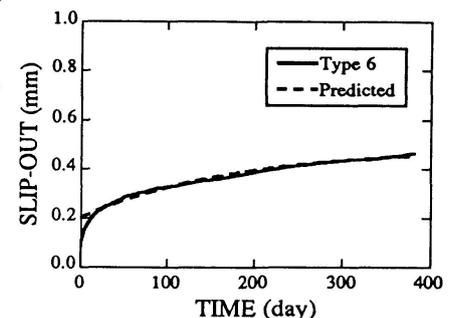
Fig.9 Predicted Time-dependent Behavior of Sockets (Method 3)

4. PREDICTION OF TIME-DEPENDENT BEHAVIOR OF A CABLE-STAYED BRIDGE

4.1 Finite Element Formulation

The equilibrium equations for the cable, tower and girder elements after applying Laplace transform leads to a linear system of equations, whose stiffness matrices K_{ij} are as presented bellow.

$$\overline{K}_{ij}(s) = \sum_{i=1}^{m} \sum_{j=1}^{n} \int_{V} B_{im} \overline{E}_{mn}(s) B_{nj} dV$$

$$(7)$$

where B_{im} and B_{nj} are strain matrices and $E_{mn}(s)$ is the elastic modulus corresponding to the Laplace space:

$$\overline{E}_{mn}(s) = \frac{s + \dfrac{E_2}{\eta}}{s + \dfrac{E_1 + E_2}{\eta}} E_1$$

for visco-elastic elements   (8-a)

$$\overline{E}_{mn}(s) = E_1$$

for elastic elements   (8-b)

The F.E.M. analysis as above described provides solutions in the Laplace space which has to be converted into the real time domain, so as to give the final solution. Therefore, an inverse transformation has to be carried out [2].

In case of cable-stayed bridges, the cables, towers and girders have different visco-elastic constants and therefore, different intervals of convergence, which makes it difficult to perform a numeric inverse transform considering, simultaneously, all the structural elements visco-elastic. Thus, the bridge analysis was carried out considering each element, separately, visco-elastic (case 1,..., case n) and the final solution was assumed to be a linear combination of all the n cases [3]. The contribution factor for each of the terms of the linear combination is determined by means of the least square scheme in the Laplace image space and the use of the Regula-Falsi method.

4.2 Model Bridge

The model bridge, as presented in Fig.10, is a cable-stayed bridge with a central span of 238.0m and the side spans supported by a PC rigid frame bridge. The structural analysis was carried out for half the bridge, considering its structural symmetry and the cables actually used in this bridge were of type 4 and type 6.

Thus, the following cases were considered for the analysis:
- case 1: only the cables are linearly visco-elastic;
- case 2: only the concrete members of the PC rigid frame bridge are linearly visco-elastic, and
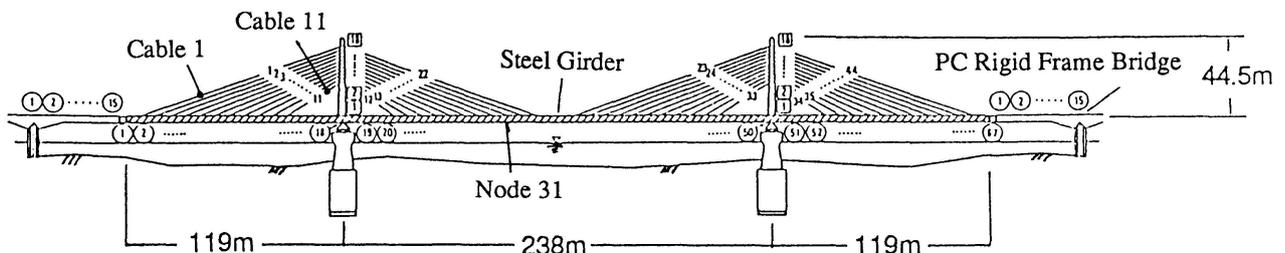- case 3: final solution assumed as a linear combination of the former cases.

Fig.10 Model Bridge

4.3 Analytical Results

The structural analysis was performed using the experimental values of the specimen types 4 and 6, which, although having the same cable material, had different types of sockets. Fig.11 presents the time variation of the axial force in cable No.1 (one of the longest cable) and Fig.12, the time variation

of the axial force in cable No.11 (one of the shortest cables). The forces stabilized in a short time, presenting similar values for both types of cables.
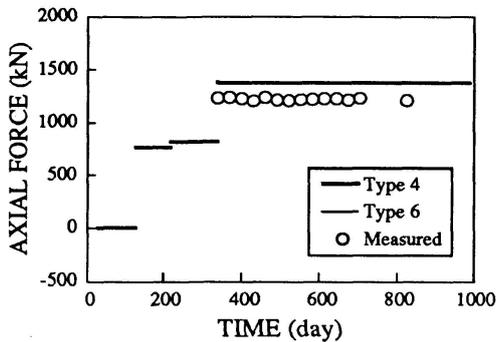
Fig.11 Variation of the Cable Force
Cable No.1 (Types 4 and 6)
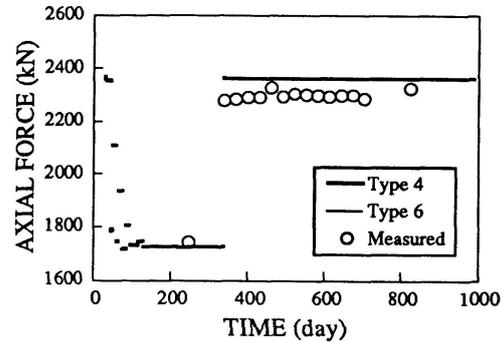
Fig.12 Variation of the Cable Force
Cable No.11 (Types 4 and 6)

On the other hand, as it can be noticed in Fig.13, the time-dependent behavior of the nodal displacements were more remarkable in type 6, whose socket is of a more sensitive type. The effectiveness of considering the cables and sockets separately in the evaluation of the visco-elastic parameters is shown in Fig. 14, where the curves for the case in which cable and sockets are considered separetly provides values closer to that of the data measured in situ.
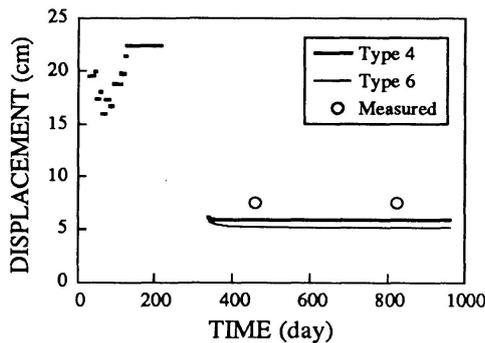
Fig.13 Displacement of Node No.31
(Types 4 and 6)
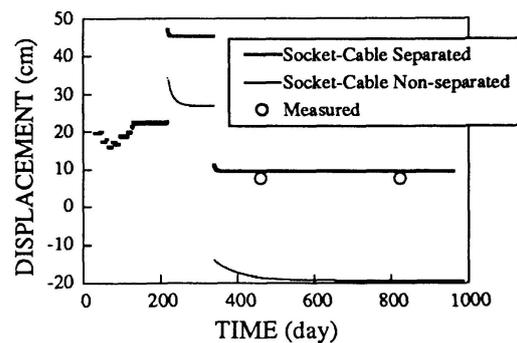
Fig.14 Displacement of Node No.31
Comparison between (i) Socket-Cable
Separated and (ii) Not Separated

A simulation was also performed using a ficticious type of cable, assuming elastic constants similar to that of type 1 (E_1=200GPa, E_2=4000GPa) and the delay-time ($T=\eta/E_2$) of 50 days, which correspond to the values of locked coiled rope [1]. Fig.15 illustrates the time-dependent behavior of the nodal displacement when using the ficticious cable.
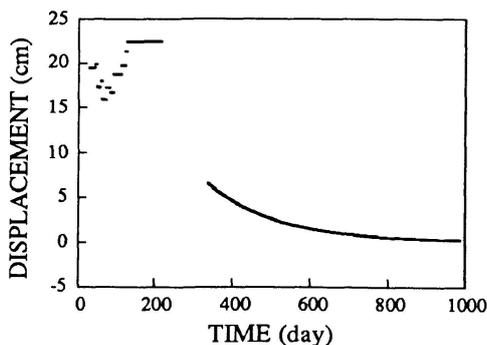
Fig.15 Displacement of Node No.31
(Ficticious Cable)
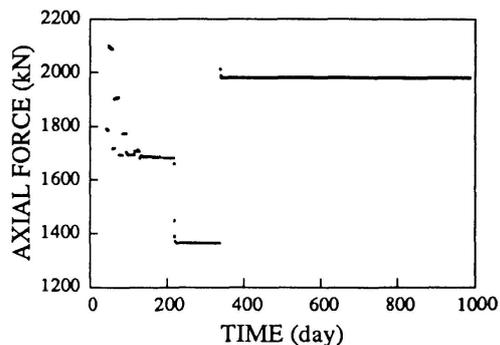
Fig.16 Variation of the Cable Force
Cable No.11 (Ficticious Cable)

Spatial Behaviour of Plate Girder Bridges under Redecking
Comportement spatial des ponts à poutres à âme pleine lors de la rénovation de la chaussée
Räumliche Wirkung von Plattenbalken-Brücken bei Fahrbahnerneuerung

S. NAKAMURA
Kawasaki Steel Corp.
Tokyo, Japan
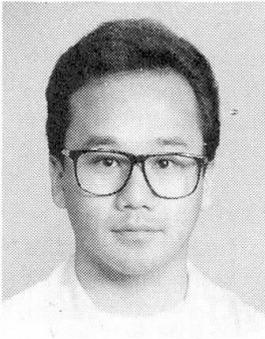
T. YAMAO
Kumamoto University
Kumamoto, Japan

Y. KAWAI
Kawasaki Steel Corp.
Tokyo, Japan

T. SAKIMOTO
Kumamoto University
Kumamoto, Japan

SUMMARY
Spatial behaviour of plate girder bridges under redecking is studied experimentally and theoretically. A series of statical loading tests were conducted under several loading and structural conditions which may occur when the bridge is partially open to traffic during redecking. A finite element method was developed in order to analyze the spatial behaviour of plate girder bridges and the results of analysis are compared with the test results. Both the displacements and the stresses obtained from these analyses show good agreement with those of tests. Validity and efficiency of the theoretical method are shown.

RÉSUMÉ
L'article présente l'étude du comportement théorique et expérimantal des ponts à poutres à âme pleine, lorsque l'on maintient la circulation sur une partie de la chaussée au cours de sa rénovation. A cet effet, ont été élaborés aussi bien une série d'essais statiques pour différents états de chargte et conditions structurales, qu'une analyse méthodique spatiale au moyen de la méthode des éléments finis. La comparaison des résultats de calculs avec ceux des mesures fait apparaître une très bonne concordance tant des déplacements que des contraintes. Enfin, l'auteur montre la validité et l'efficience de cette méthode de calcul.

ZUSAMMENFASSUNG
Theoretisch und experimentell wurde die räumliche Wahrung von Plattenbalken-Brücken studiert, wenn infolge Fahrbahnerneuerung nur Teile für den Verkehr geöffnet sind. Zu diesem Zweck wurde eine Serie statischer Belastungstests für mehrere Last- und Tragwerkszustände sowie eine Methodik zur räumlichen Analyse mittels Finite-Elementen entwickelt. Beim Vergleich der Rechen- mit den Messergebnissen zeigt sich eine gute Übereinstimmung in den Verschiebungen und Spannungen. Validität und Effizienz des Berechnungsverfahrens werden aufgezeigt.

1. INTRODUCTION

In recent years, many reinforced concrete (RC) floor slabs of highway bridges have been deteriorated or damaged and require rehabilitation, repair and replacement. This is caused by the increase in traffic volume and the illegal passing of over-loaded heavy vehicles. Although many studies have been reported in reference to the repairing or strengthening method of damaged RC floor slabs, the redecking method by orthotropic steel deck has become of major interest in the view of the reduction of the dead load and the expected remaining life of bridge lately[1,2]. The authors have been studied the useful method of replacing damaged floor slabs with the prefabricated steel deck of Battledeck Floor Type[3] which is easily manufactured[4,5]. The bridge has to be partially open to traffic because a long traffic close of bridges with heavy traffic is usually not allowed in the work of replacing. Therefore, it is important to clarify the spatial behavior as a whole system and local stresses of plate girder bridges during the redecking.

This paper presents the results of statical loading tests for a large scale model and the finite element analysis for plate girder bridges. In the analysis, the RC floor slab is modelled by thin plate elements having six degrees of freedom for one node and the main girder by equivalent substituted truss system. The supporting cross beam and the cross frame are modelled by beam-column elements. Since the shear connector transfers the load primarily by shear, it is assumed that their flexural and torsional stiffness can be neglected. Validity and efficiency of the theoretical method are examined by comparing with the experimental results. Many useful information for redecking design are obtained from the results of tests and analyses.

2. SUMMARY OF LOADING TEST

2.1 Test model

Although the test model is designed to simulate the replacement of a damaged RC floor slab with the steel deck, a bridge model with the steel deck in place of the RC floor slab is used here. This is due to the practical reason that the thin concrete slab in the model may cause the structural unbalance between the floor slab and steel girders and it may be difficult to conduct the casting and removing operations of the RC floor slab in the testing frame.

The bridge model is composed of three main girders, the prefabricated steel deck, supporting cross beams and cross frames. The steel deck used is the Battledeck Floor Type with welded longitudinal ribs as shown Fig.1 and is connected by high strength bolts to the main girders. In order to simulate the behavior of the actual bridge under redecking, the steel deck is divided into two panels along the length. The supporting cross beam is corresponding to the transverse rib of the orthotropic steel deck and is fastened by high strength bolts to main girders.

2.2 Test procedure

The objectives of the experimental programme are to investigate the spatial structural behavior of the girder bridges as a whole system and the local stress during the redecking. The statical load is applied at the centre of the span through 300mm x 120mm hard rubber plates which are placed on the steel deck. The loading conditions and the applied load are summarized in Table 1. The test procedure corresponding to the actual replacement of the RC floor slab with the steel deck is selected and consists of a total of seven steps as shown in Table 2. The models of STEP 1 & 2 are composed of three main girders and
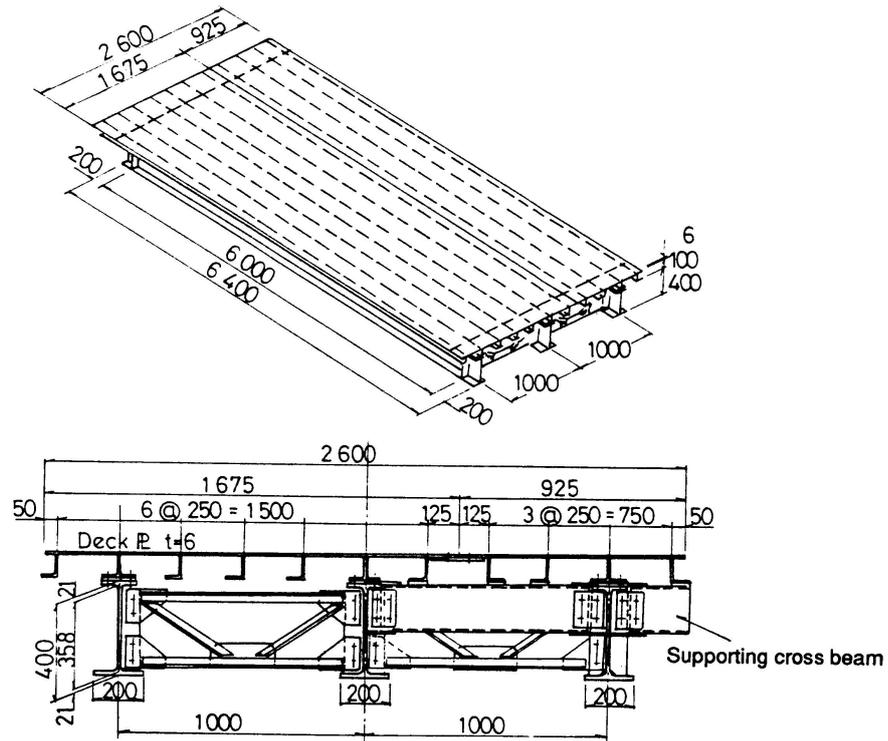
Fig. 1 General layout of the bridge model

Table 1 Loading cases

	Max. Load (kN)	Loading Conditions
CASE I	150	
CASE II	70	
CASE III	100	
CASE IV	150	
CASE V	70	

Table 2   Test procedure

		Loading Conditions
	STEP 1	CASE I ≀ CASE III
	STEP 2	CASE I ≀ CASE III
	STEP 3	CASE I ≀ CASE V
	STEP 4	CASE I ≀ CASE V
	STEP 5	CASE I ≀ CASE V
	STEP 6	CASE I ≀ CASE V
	STEP 7	CASE I ≀ CASE V
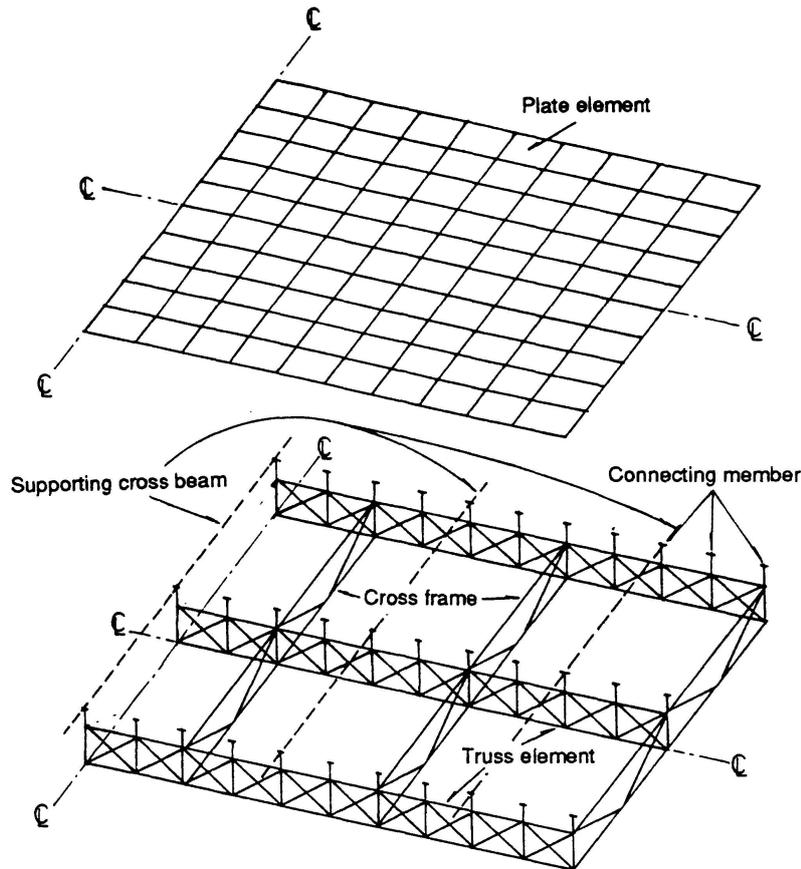
Fig. 2   Theoretical model

cross frames without the steel deck, and for the model of STEP 2 supporting cross beams are installed in addition to cross frames. Measurements of strains in the main girders, steel deck and supporting cross beams were made by using strain gages. The deflection of the steel girders and the shear slip between the deck plate and the main girder were measured using electrical and cantilever type displacement meters, respectively.

3. SUMMARY OF ANALYSIS

3.1 Theoretical model

The theoretical model used for the analysis of the plate girder bridge which composed of steel deck, main girders, supporting cross beams and cross frames is shown in Fig. 2. The steel deck is modelled by triangular thin plate elements having six degrees of freedom for one node. The stiffness matrix of the plate element is derived with the consideration for in-plane flexural stiffness[6]. The supporting cross beam is modelled by thin-walled beam-column elements[7] and the cross frame by truss elements. The main girder is modelled by an equivalent truss system which can store the same amount of strain energy with that stored in the plate girder. With reference to Fig. 3, the cross sectional areas of the substituted truss members are given by the following equations[8]:

Upper chord member: $Acc = \dfrac{I}{(hc+ht)hc}$

Lower chord member: $Act = \dfrac{I}{(hc+ht)ht}$

Vertical member: $Av = \dfrac{6AwG}{\mu E\tan\theta}$

Diagonal member: $Ad = \dfrac{3AwG}{2\mu E\sin\theta\cos^2\theta}$
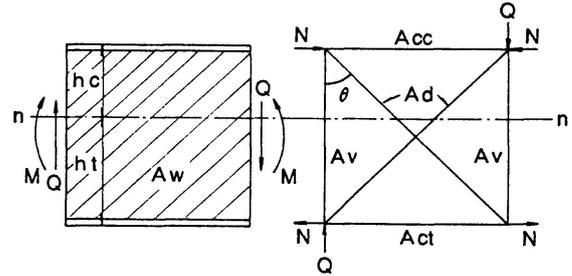
Fig.3 Substituted truss

where I is the moment inertia of the girder cross section about the neutral axis, ht and hc are the distances from the neutral axis to each outermost fiber, respectively, E and G are the Young's modulus and the shear modulus, μ is the shape factor and Aw is the cross sectional area of the web plate. Though the steel deck is connected by high strength bolts to main girders, the shear connector is modelled by cantilever elements which permits only the horizontal shear at the free end of element.

3.2 Computation method

The computation was carried out for the half of the girder bridge considering the symmetrical condition at the midspan. The deck plate is divided into 10 elements both along the length and the width of the deck. In the modeling, the cross sectional shape of the theoretical model is used the rectangular determined according to the condition that the flexural stiffness of the deck plate section equals those of experimental model. The bridge , part of which steel deck is removed, is modelled in the same way, but the thickness of deck plates supposed to be removed is assumed to be negligibly small (0.001cm) in the analysis.

4. RESULTS AND DISCUSSIONS

4.1 Load distribution effect of cross frames and supporting cross beams

The load distribution effects of cross frames and supporting cross beams are examined at the test steps 1 & 2 (without the steel deck) for the loading CASE I ~ III.
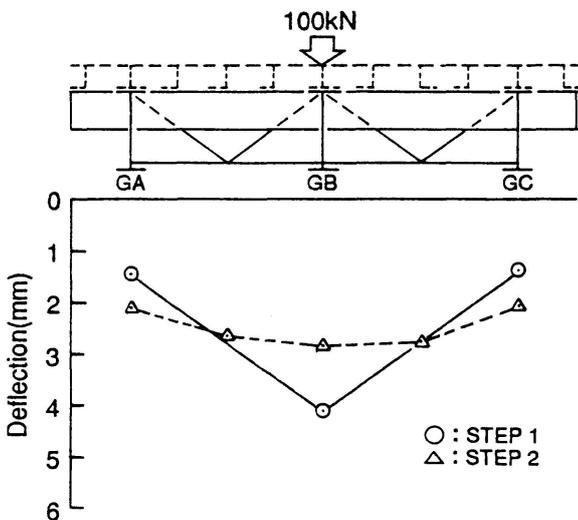
Fig. 4 Deflection of main girders at midspan
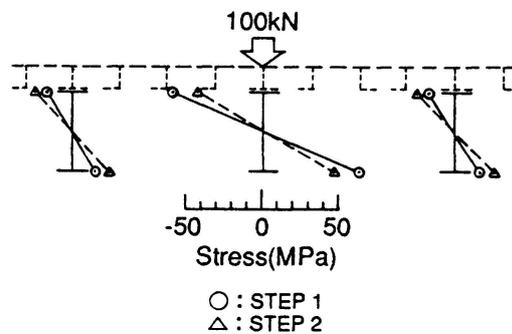
Fig. 5 Stress distribution of main girders at midspan
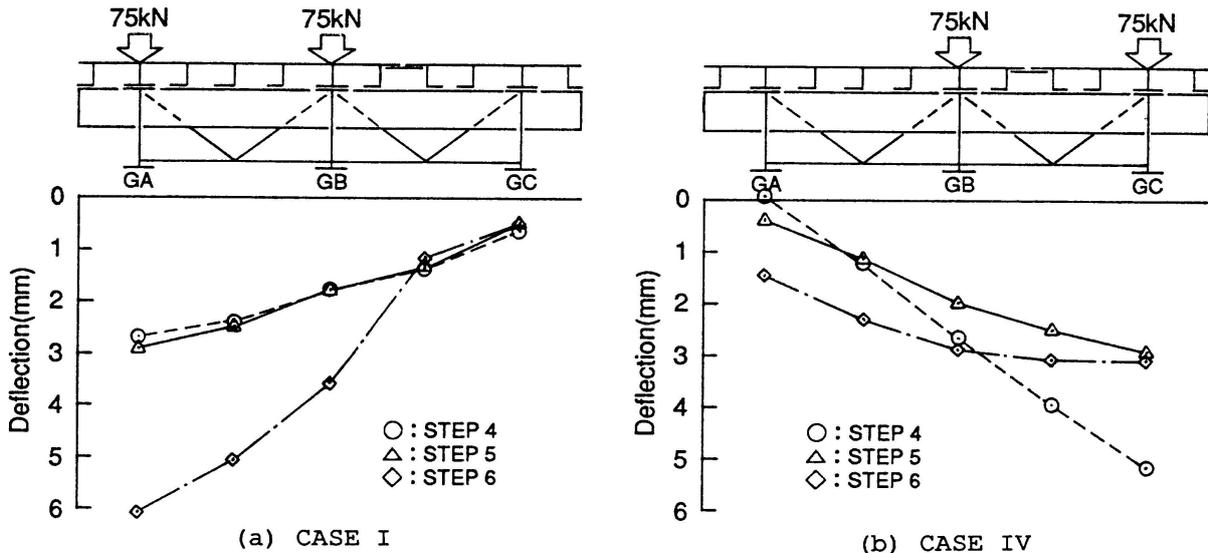
Fig. 6 Deflection at midspan for each STEP
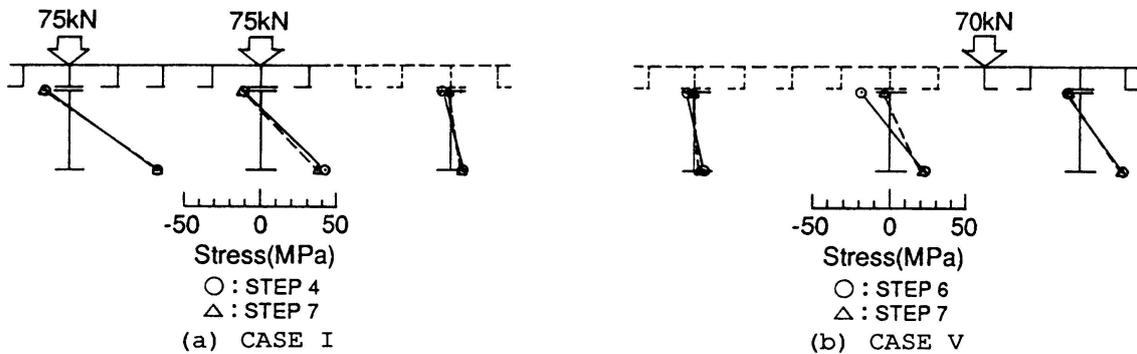
Fig. 7 Distribution of normal stresses at midspan

Figs. 4 and 5 show the deflection at midspan and the distribution of normal stresses on the girder under concentrated load at the midspan, respectively. It can be seen that 40% of the applied load is distributed to the exterior girders by using cross frames(STEP 1) and for the model of STEP 2 by using supporting cross beams in conjunction with cross frames 50 ~ 60% of the applied load is distributed to the exterior girders. From these test results, we can recognize that the use of supporting cross beams in the prefabricated steel deck system can give large effects of the load distribution.

4.2 Behavior during redecking

The deflection at midspan subjected to a lateral load at the midspan for STEP 4~6 are shown in Fig. 6. It may be found that the deflection for STEP 4 in CASE IV and STEP 6 in CASE I are larger than those of the other loading cases. This is due to the reason that the loads are directly applied to the main girders where part of the deck plate is removed. Fig. 7 shows the distribution of normal stresses on main girders at midspan for STEP 4,7 in CASE I and STEP 6, 7 in CASE V. By comparing the stress in the low flange of main girders with (STEP 7) and without (STEP 6) the deck plate, we notice that the stress of main girder without a part of deck plate is relatively small and is nearly equal to those of a complete system (STEP 7). The reason of this is that the moment inertia of the composite section is 2 ~ 3 times larger than that of a main girder and this section is mainly in charge of the applied load. From test results, it can be noticed that the supporting cross beams play satisfactory

Table 3 Comparison of test and
analysis for each slip modulus k

(a) Deflection   Unit:mm

		GA		GB		GC
Experiment		0.90	1.32	1.42	1.31	0.94
Analy-sis	k=9.8	0.86	1.16	1.31	1.16	0.86
	98	1.16	1.31	1.48	1.31	1.16

(b) Stress   Unit:MPa

		GA		GB		GC	
		Comp	Tens	Comp	Tens	Comp	Tens
Experiment		5.2	16.5	12.2	34.4	4.8	15.8
Analy-sis	k=9.8	3.8	16.0	9.2	34.1	3.8	16.0
	98	6.0	17.0	16.6	34.8	6.0	17.0

100kN

-50   0   50
Stress(MPa)

	Experiment	Analysis
STEP 3	△	— —
STEP 4	○	——
STEP 6	◇	- - -
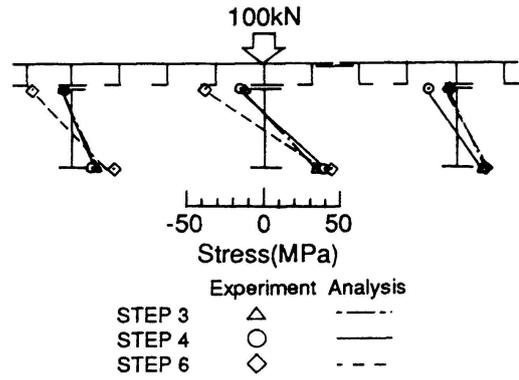
Fig. 9 Stress distribution at
midspan

(a) CASE I

(b) CASE II
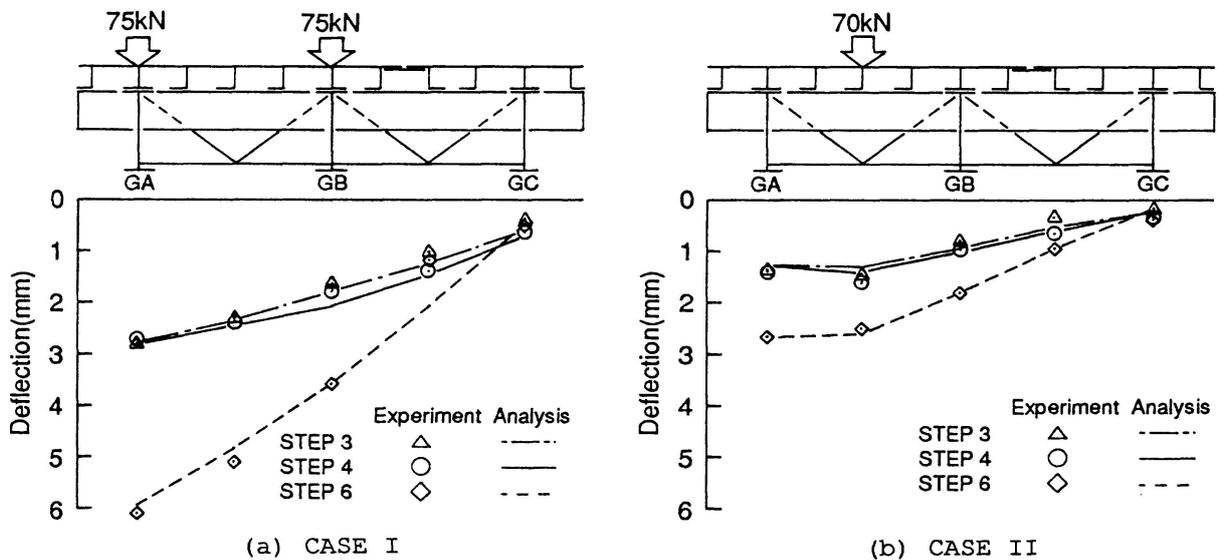
Fig. 8 Comparison of deflection at midspan between theory and experiment

role for the load distribution in transverse direction together with for the
outer girder without the deck.

4.3 Comparison of tests and theory

To determine the slip modulus k of the shear connector prior to model analysis,
the complete models (STEP 3) subjected to a lateral load at midspan were
analyzed for two k values, k= 9.8 and 98 (N/m/m), based on the previous studies
[4,5]. The comparisons of tests and the theory for deflection and stress of
main girders are given in Table 3. The slip modulus k= 9.8 (N/m/m) was adopted
in this analysis because it tends to give overestimated conservative results in
comparison with test results. The deflection at the midspan for STEP 3~6 in
CASE I and II are shown in Fig. 8. Though the small differences between the
theoretical and experimental results for STEP 6 in CASE I is observed, it can
be noticed that the good agreement exists between the two sets of results.
Fig. 9 shows the normal stress distributions on three main girders at the
midspan for CASE III. The theoretical results correspond to the experimental
results quite well. In spite of small differences for some loading cases, it
can be seen that the results of the present analysis have fairly good
correspondence with the test results as a whole. The validity of the present

method can be recognized. This numerical method will be utilized to investigate the spatial behavior of existing plate girder bridges under redecking.

5. CONCLUSIONS

Spatial behavior of plate girder bridges under redecking is studied experimentally and theoretically. From this study the following conclusions can be drawn.

1) The redecking procedure of actual bridges with deteriorated RC slabs is simulated well by the experiment.
2) It is recognized that the use of supporting cross beams in the prefabricated steel deck system can give large effects of the load distribution.
3) In spite of small differences for some loading cases, it can be seen that the results of the present analysis show good agreement with the test results as a whole. The validity of the present method can be recognized.
4) The present method will be utilized to investigate the spatial behavior of existing plate girder bridges under redecking.

REFERENCES

1. WOLCHUK R. , Applications of Orthotropic Decks in Bridge Rehabilitation, Engineering Journal. 3rd Qtr., 1987.
2. Bridge Design Department Ishikawajima-Tekko Construction Co. Ltd. , The Work of Replacement of Reinforced Concrete Slab of "Shin-Kannon Bridge" for Chougoku Regional Construction Bureau, Ministry of Construction. Ishikawajima-Harima Engineering Review, Sep., 1985. (in Japanese)
3. A.I.S.C. , Design Manual for Orthotropic Steel Plate Deck Bridges.
4. FUJIWARA M., HARA M., YOSHIDA H. and KAWAI Y., Basic Experiments on Pre-fabricated Steel Deck for Redecking. Proc. of 43th Annual Conference of JSCE, Oct., 1988. (in Japanese)
5. MURAKOSHI J., KAWAI,Y., YOSHIDA H. and NAKAMURA S., Statical Loading Tests and Fatigue Tests on Prefabricated Steel Deck for Redecking using large scale models. Proc. of 44th Annual Conference of JSCE, Oct., 1989. (in Japanese)
6. YAMAO T. and SAKIMOTO T., Nonlinear Analysis of Thin-walled Structures by a Coupled Finite Element Method. Eng./Earthquake Eng., Vol.3, No.2, Oct.,1986. (in Japanese)
7. YAMAO T., SAKIMOTO T., YUJI S. and KAWAI Y., Analysis of a Plate Girder Bridge with a Reinforced Concrete Slab. IABSE Symposium Brussels 1990, Sep., 1990.
8. YAMAO T., SAKIMOTO T., SHIIHARA K., KAWANO K. and KAWAI I., An Analysis of the Behavior of Crane Girders using an Equivalent Substituted Truss. Journal of Structures and Materials in Civil Engineering, Vol.5, Jan., 1990. (in Japanese)

Method for Evaluating the Load Carrying Capacity of Existing Bridges
Méthode d'evalution de la capacité portante des ponts
Eine Methode zur Tragfähigkeitsbewertung bestehender Brücken

Souxin WU
Doctoral Student
Southwest Jiaotong Univ.
Chengdu, China

Yuanchang LAO
Professor
Southwest Jiaotong Univ.
Chengdu, China

Souxin Wu, born 1966, received his M.S. degree at Southwest Jiaotong Univ. He is now involved in finite element analysis of concrete structures and evaluation of existing bridges.

Yanchang Lao, born 1920, received his Ph.D. at Imperial College of Science and Technology in U.K. He is now involved in assessment of structural capacity.

Dayuan SHEN
Professor
Southwest Jiaotong Univ.
Chengdu, China

Yalin PEI
Lecturer
Southwest Jiaotong Univ.
Chengdu, China

Dayuan Shen, born 1932, graduated from Tangshan Jiaotong Univ. He is now involved in research on concrete bridges.

Yalin Pei, born 1958, received her M.S. degree from Southwest Jiaoton Univ. She is now involved in finte element analysis of concrete structures.

SUMMARY
On the basis of inspection, testing and analysis for a number of existing bridges, the factors which have influence on the load carrying capacity of existing reinforced concrete bridges are identified and a finite element model for evaluating the load capacity is developed. A simulation method for the evaluation is proposed, by which the load testing of bridges can be simulated by means of computers and the characteristics of the load carrying capacity of existing bridges can be calculated.

RÉSUMÉ
Sur la base d'inspections, d'essais et d'analyses d'un grand nombre de ponts, les facteurs qui influencent la capacité portante des ponts en béton armé ont été identifiés et un modèle par éléments finis a été développé. Une méthode de simulation pour l'évalution est présentée, par laquelle l'essai de charge du pont peut être simulé au moyen de l'ordinateur; les caractéristiques de la capacité portante des ponts peuvent être ainsi également calculées.

ZUSAMMENFASSUNG
Auf Grund der Untersuchungen, Proben und Analysen von zahlreichen bestehenden Brücken werden die Hauptfaktoren, die Einfluss auf die Tragfähigkeiten von bestehenden Stahlbetonbrücken ausüben, festgestellt und ein Finite-Elemente- Modell für die Tragfähigkeitsbewertung entwickelt. Mittels dieser Methode kann die Belastungsprobe der Brücken mit Hilfe von Computern simuliert und dadurch können die Kennziffern der Tragfähigkeit von Brücken berechnet werden.

1. INTRODUCTION

With the development of transportation, the load carrying Capacity of a number of existing bridges are found to be insufficient due to progressing deterioration and increased loads. There are nearly 136,000 highway bridges in China, About 5,000 of these are judged to be functionally obsolete or inadequate for current requirements, the service age of these bridges are ranged from 30—years to 40—years. In addition, some of bridges constructed over the last 20 years are considered to be structurally deficient because of deterioration or distress[1][2].

While replacing all the deficient bridges mentioned above with new bridges is often extremely difficult and expensive, a moderate increase of structural capacity through rehabilitation and repair is fairly cheap and easy to obtain. To avoid high costs of rehabilitation and repair, the evaluation of the bridges must accuratelly reveal the present load carrying capacity and any further changes in the capacity in the applicable time span. In recent years, many method for evaluating the load carrying capacity of existing bridges have been developed. these method can be roughly divided into three kind: Knowledge —based method; computalional method; and load testing method. The knowledge—based method has the advantage of assessing the damage state of the bridges, but can not give exact index about the load carrying capacity. Most computational methods are similar to design methods, the hypothesis on which design methods based are not quite the same as practical behavior of existing bridges, and computational results may be doubtful. load testing on bridges can directly examine the load capacity and the results are more reliable than other methods. However, it would be very expensive to test all the deficient bridges. In order to explore the load carrying capacity of existing bridges, it is necessary to develop an inexpensive evaluation method which can fully take into account the real behavior of existing bridges and give reliable results about the load capacity.

The objective of this paper is to identify the factors which affect the load carrying capacity of the bridges and develop a simulation method for the evaluation. Using the method, the load testing of the bridges can be simulated by means pf computers and the index about the load carrying capacity can be caculated. An example of evaluating a T-beam bridge is also presented.

2. FACTORS AFFACTING THE LOAD CAPACITY OF R. C. BRIDGES

Over the years of servicing, various forms of deterioration would appear on beams, piers and bases of bridges and all affect the load carrying capacity. So the load carrying capacity include the capacity of upper structure which composed of beams and deck and that of lower structure constituted by piers and bases. Only the upper structural capacity is studied in this paper.

In order to assesss the damage state of old bridges and identify the factors which affect the load carrying capacity of the bridges, a thorough field survey of old R. C. bridges located in Guangdong province in China was made and static and dynamic load tests were performed on some of these bridges[3]. Inspection and testing show that the deterioration emerged on beams and deck are main factors which influence the load carrying capacity. The deficiencies on the attachment such as discharge orifices and expansion joints results in the damages on beams and deck, then have indirect influence on load capacity. Various types of deterioration -efflorescence, leakage, cracking and spalling-can contribute to the reduction of bridge's load capacity to different degree. Ignoring the deficiencies which have little influence on the load capacity and only beams and deck are considered, main factors affecting the R. C. bridge's load capacity can be identified as shown in Fig. 1.

Among the factors, cracking of concrete is very important to estimate the load capacity. The density, width, length and pattern of cracks are significant indexes for the estimation. The factors given in Fig. 1 must be take fully into account in the computational model for evaluation of R. C. bridge' s load carrying capacity.
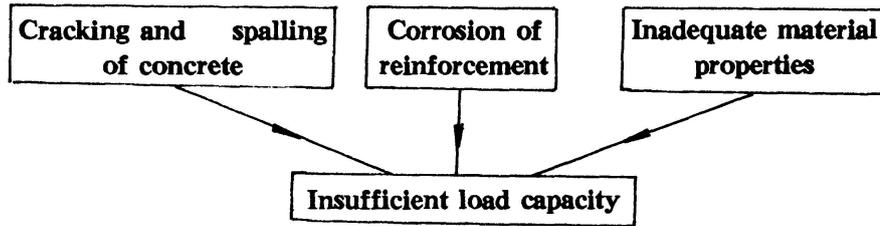
Fig. 1 Main factors affecting load capacity

3. COMPUTATIONAL MODEL FOR R. C. BRIDGE' S LOAD CAPACITY

3. 1 Mathematical Model

Theoretically, for a given loadings and structure type, a bridge' s load carrying capacity can be determinated in terms of the parameters such as load components, dimensions, strength of materials, etc. The evaluation philosophy of an existing bridge must differ from the design philosphy of a new bridge. In this study, the load carrying capacity index, R , is defined as follows:

$$R = g[s(t), f(t), x(t), \varphi(t)]$$
(1)

where $S(t)$ represents load effect; $f(t)$ represent strength of materials; $x(t)$ represent dimensions; $\varphi(t)$ is structural integrity and is equal to $(1 - d)$, in which d is damage. All of these parameters are functions of service time t . Assuming that, R is differentiable continuous function of all the parameters, the change of load capacity, $\triangle R$, can be derived from Eq. (1) as:

$$\triangle R = (\partial g/\partial s)\triangle s + (\partial g/\partial f)\triangle f + (\partial g/\partial x)\triangle x + (\partial g/\partial \varphi)\triangle \varphi$$
(2)

in which $\triangle s$, $\triangle f$, $\triangle x$ and $\triangle \varphi$ denote the changes of load effect, strength of materials, dimensions and structural integrity, respectively. Over the years of performance, the actual load carrying capacity, R_t , at the time of evaluating, t , is witten as:

$$R_t = R - \triangle R$$
(3)

The resistance coefficient, k , can be defined as:

$$K = (R_t - G)/S$$
(4)

where G represents dead load effect; S represent the effect of the live loads used for evaluation.

3. 2 Finite Element Model

To reveal the real load carrying capacity of bridges, a rational computational model must be established. Actual behavior and the factors affecting the load capacity must be fully considered in the model. The finite element method is appropriate for dealing with non — homogeneous materials, nonlinear constitutive relationships and complicated boundary conditions. It is easy to dispose

deterioration or distress which contributes to reduction of the load capacity by using the finite element method. Thus a finite element model can be developed to caculate the load carrying capacity index, R . The major factors in Fig. 1 can be taken into account in the finite element model and constitutive relationships(Fig. 2)

Fig. 3(a)shows a damaged simply supported T—beam, which has four cracks located at A, B, C,and D, respectively. Spalling occurs at location E, and result in corrosion of parts of reinforcing bars. Meanwhile, expansion bearing lose its efficacy. Finite element model of the beam is illustrated in Fig. 3. (b). Details of the model will be described in the following.
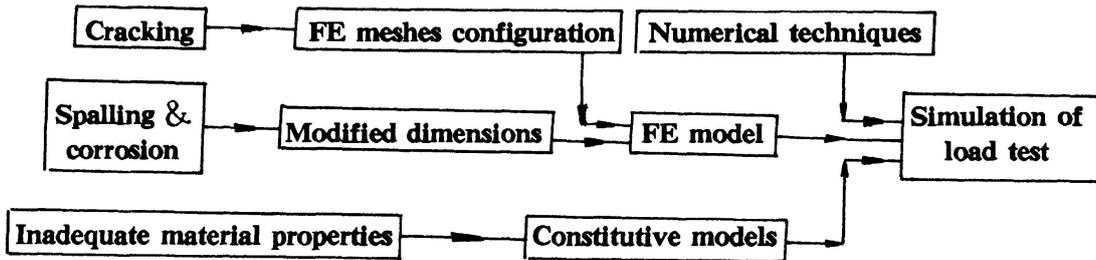
Fig. 2 Management of the factors affecting load capcity

(a) Deteriorated beam

(b) Finite Element Idealization
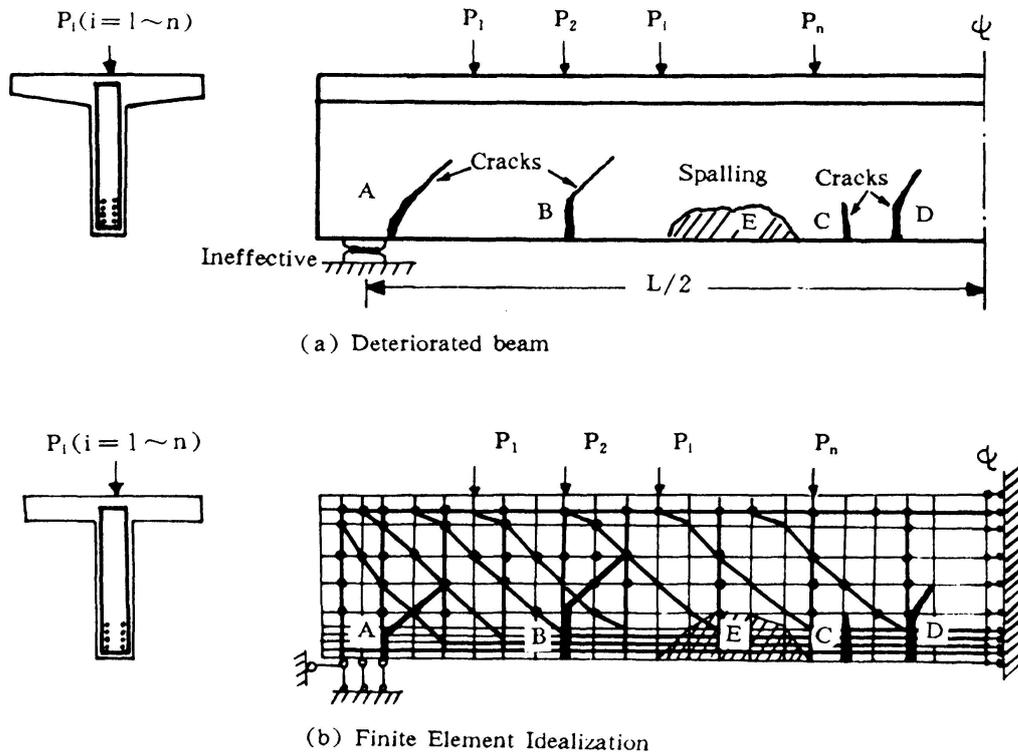
Fig. 3 Finite element model of deteriorated beam

3. 2. 1 Concrete

The assumption of the plane stress is considered to be reasonable for T—beam subject to loadings in— web plane. Reduction of concrete section due to spalling is taken into account by the modified element

thickness, T_c , defined as:

$$T_c = K_c T \tag{5}$$

where K_c is modification coefficient, T is original thickness.

Existing cracks are modelled with two techniques: Discrete model and smeared crack model. The discrete model approaches a single fully separative crack by disconnecting nodal points (Fig. 4(a)). Interlock elements are placed across the incompletely separative cracks to simulate aggragate interlock (Fig. 4(b))

(a)   (b)
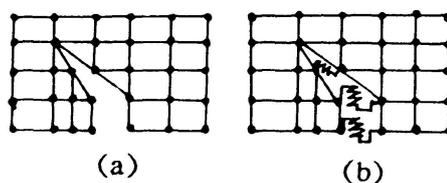
Fig. 4 Discrete crack model

The smeared crack model represent overall influence of many discrete cracks existing in the domain of the element. the constitutive eqation is expressed by[8]:

$$\begin{bmatrix} d\sigma_1 \\ d\sigma_1 \\ d\sigma_1 \end{bmatrix} = \begin{bmatrix} E_1 & 0 & 0 \\ 0 & E_2 & 0 \\ 0 & 0 & G_{cr} \end{bmatrix} \begin{bmatrix} d\varepsilon_1 \\ d\varepsilon_2 \\ d\gamma_{12} \end{bmatrix} \tag{6}$$

where G_{cr} is reduced shear modulus which reflects the density, width and degree of separation of the cracks.

3. 2. 2 Steel reinforcement

Main reinforcing bars are represented by axial force elements with two translational degrees of freesom defined at each node. Corrosion of rebars is considered by reduction of the cross sectionl area of the bars. Secondary reinforcement, such as stirrups is assumed to be distributed over concrete elements and forms composite concrete — steel element. The material stiffness of the element is defined as follows [8]:

$$[D] = [D^c] + \sum_{i=1}^{n}[D_i^s] \tag{7}$$

where $[\ D^c\ ]$ and $[\ D_i^s\ ]$ are the concrete and reinforcement material stiffness matrices, respectively.

3. 2. 3 Bond between steel reinforcement and concrete

If the influence of bond slip is considered, linkage elements must be set up to model bond behavior, so the number of nodal points will increase greatly. For the sake of utilizing memory capacity of computer

effectively, reinforcement may be assumed to be connected directly to the concrete at the nodal points.

4. CONSTITUTIVE RELATIONS FOR THE CONSTITUENT MATERIALS

Material properties have a significant influence on the load capacity. Actual material parameters must be used in constitutive relations. Biaxial nonlinear constitutive relations and failure theories should be applied to explore the realistic load capacity of existing bridges.

The concrete constitutive model and failure crireria of Balakrishnan & Murray[5] are introduced in this study. The model divides the uniaxial response curve for concrete into five damage regions described as linear elastic; compressive strain hardening; compressive strain softening; tensile strain softening; and tensile stiffening regions. When used under biaxial stress conditions, the model is considered orthotropic after cracking. The effect of biaxial stress conditions on peak strength is represented by a variation of the Kupfer — Hilsdorf failure curve in stress space in which the compressive and tensile envelopes are separatelly specified[4][5]. In the tension—compression region, tensile stress less than $0.5 f_t$ does not reduce compressive strength. If $\sigma_1 > 0.5 f'_t$, the ultimate strength may be described as:

$$f_{tu} = 2f'_c/(1/2 + 2f'_c/f'_t) \tag{8}$$

$$f_{cu} = (-1.5 + f_{tu}/f'_t)|f'_c| \tag{9}$$

In compression—compression region, the ultimate compressive strength may be written as:

$$f_{cu} = (1 + 3.65)f'_c/(1 + a)^2 \tag{10}$$

in which $a = \sigma_1/\sigma_2$, σ_1 and σ_2 are major and minor principal stresses respectively, f_{cu} and f_{tu} are peak compressive and tensile stresses respectively. Details of the model are described in reference[5]. The paramefers in the model such as cylinder compressive strength f'_c, elastic modulus E, should be determined with nondestructive inspection such as sonic pulse velocity measurements. If neccessary, cores are taken from bridge for compressive and split test.

Reinforcing steel is assumed to be elastic perfctly plastic material. Actual values of the yield strength f_y and elastic modulus E_s are used. The strain—hardening region may be considered, if neccessary.

The bond stress—slip relationships of Mirza and Houde is used, expressed as[6]:

$$\tau = (54 \times 10^2 S{-}25.7 \times 10^5 S^2 + 5.98 \times 10^8 S^2{-}0.558 \times 10^{11} S^4 \sqrt{f'_c/41.5}) \tag{11}$$

in which τ is the bond stress in MPa, S is the slip in cm.

Interlock elements are employed to model the interface shear transfer across the crack by aggragate interlock and friction. The stiffness of the element is derived from Horde & Mirza's shear stress-displacement relation as[6]:

$$Kg = 63.85(1/C)^{3/2} \sqrt{f'_c/35A} \tag{12}$$

in which A is the area for which one element is responsible, in cm^2; f'_c in MPa; C is crack width in cm; k_g in N/cm.

5. EVALUATING PROCEDURE

Based on the mathematical model and the finite element model aforementioned, a finite element program can be developed and implemented into a particular computer code to simulate the load tests of R. C. bridges. For T—beam bridges, each beam of the bridge is evaluated as a single unit. Simulation results of all beams are synthesized and analyzed to give the resistance factor of the whole bridge. The evaluating procedure is described in the following.

5. 1 Field Survey and Review of Design Documents

A thorough field survey is needed to obtain the information about deterioration of the bridge, including crack location and size, corrosion of reinforcement, actual material properties, and as — built dimensions. The presence and location of reinforcement can be determined though review of design documents. If the design drawings are not available, the reinforcement location may be determined using a pachometer which locate steel magnetically. The parameters needed in the computational model can be defined through field survey and review of design documents.

5. 2 Determination of Loading pattern and Finite Element Meshes

According to loads for evaluation, the most detrimental loading pattern can be decided. The transverse distribution of loads must be taken into account to determine the detrimental loading pattern applied to each beam evaluated. Generally for simply supported beam, the internal forces such as bending moments and shear forces at beam ends and mid—span control the position of loads. After defining the load pattern, finite element meshes are constructed. Data file are prepared and inputed into computer to start simulation of load test using incremental load procedure described in the next.

5. 3 Incremental Loading

For the i th T-beam, the loading factor is defined as w_{ij} in the j th loading increment. If failure occurs or the specified indexes, such as deflection and crack width, are reached at m th loading increment. The resistance coefficient for the beam is defined as:

$$K_i = \sum_{j=1}^{m} W_{ij} \tag{13}$$

5. 4 Evaluating the Load Carrying Capacity

If the bridge consist of n of beams and the resistance coefficient for every beam is caculated, the resistance coefficient of the bridge is given as:

$$K = \varphi_T \cdot Min(K_1, K_2 \cdots, K_n) \tag{14}$$

where $\varphi_T = 1 - d_T$, φ_T and d_T are integrity and damage of the transverse diaphragms, respectively; k_i (i

$= 1,2, \cdots n)$ is the i th beam's resistance coefficient.

If $k > 1$, the load carrying capacity of the bridge is enough to meet the need of present traffic. Otherwise, repairs or rehabilitation must be made to restore or increase the load capacity.

6. EXAMPLE OF BRIDGE EVALUATION

Using the computational model given is this paper, a computer program RCBM for simulaing the load tests of R. C. bridges is developed. The proposed approach is illustrated by an example. The load capacity is evaluated for one beam of a T-beam bridge which is located in chengdu city in China. The bridge, built in 1961, is a three-span simply supported T-beam bridge. The cross section are composed of 12 T-beams. The span length is 16. 3m. The mid-span cross section of one beam is shown in Fig. 5. There are 14 main unnotched rebars which have diameter of 32mm. Concrete design compressive strength is 18. 4MPa. A field survey was conducted. Spalling, corrosion of rebars, several inclined and vertical cracks were found. Actual concrete compressive strengeh is only 8. 3Mpa. One beam was taken from the bridge for failure test in order to judge whether the load capacity is enough or not. The load pattern is shown in Fig. 6 [7].
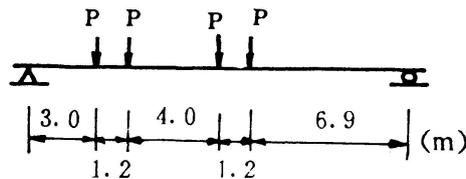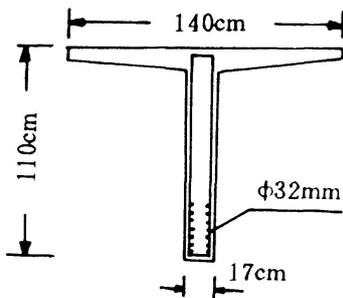
Fig. 5 Mid—span cross section   Fig. 6 Loading pattern

The design load p is 70. 5KN, corresponding to the bending moment of 782. 6KN—M in mid—span. The program RCBM is employed to simulate the failure test and evaluate the experimental results as shown in Table 1. The load—mid-pan defletion curves of the beam are shown in Fig. 7. It can be seen, from Table 1 and Fig. 7, that the proposed simulation method gives a good approximation to failure test of the T—beam, the evaluation resuts are available.

Table 1 Comparision of simulation results with test results

	Max. Load (4P) (KN)	Mid—span bending Moment (KN—m)	The resistance coeffcient
Design	282	782. 6	
Simulation	540	1497	1. 91
Test	600	1665	2. 13
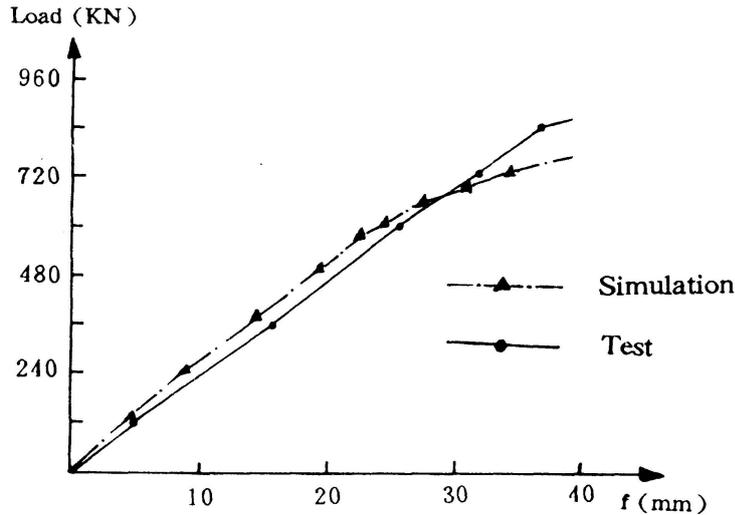
Fig. 7 Load—mid-span deflection curve

7. CONCLUSIONS

—An evaluation method for load carrying capacity of existing bridges should distinct from methods in design of new bridges. A finite element model for evaluating the load capacity is developed, in which the factors influencing the load capacity are taken into account. Nonlinear constitutive relationships and failure criteria under biaxial stresses are employed to explore the realistic load carrying capacity.

—A simulation method is proposed to estimated the load capacity of existing bridges. Using the method, load tests can be simulated in order to given reliable resistance coefficient of the bridge. The method is effective and inexpensive, since it may replace many load tests. Although the present approach is developed for R. C. bridges, it can be used in the evaluation of various types of bridges, such as steel bridges and composite bridges.

REFERENCES

1. " Inspection, Evaluation and Rehabilitation of Old Bridges," Special publication, Scientific & Technical Information Institute, Ministry of Transp. and communications, China, June 1986. (in Chinese)

2. Lou, Zhanghong, "Evaluation, Rehabilitation and Replacement of Existing Bridges," proc. of the 1987 symposium, Bridge and Structural Engrg. Division comttee of China Highway and Transp. Society , 1987. (in Chinese)

3. Wu, Souxin," Research on Nolinear Finite Element Method for Evaluating the Load Carrying Capacity of Existing R. C. Bridges," M. S. thesis, Southwest Jiaotong University, Chengdu, China, 1990. (in Chinese)

4. Kupfer, K. , Hilsdorf, H. K. , and Rüsch, H. ," Behavior of Concrete Under Biaxial stresses," Journal of ACI, No. 8, Aug. 1969.

5. Balakrishnan, S. , Murray, D. W. ," Concrete Constitutive Model For NLFE Aualysis of Structures," Journal of Structurl Engineering, Vol . 114, No. 7, July 1988.

6. Houde, J. , Mirza, M. S. , "A Finite Element Analysis of Shear Strength of Reinforced Concrete Beams," ACI 《Shear in Reinforced Concrete 》SP42, vol. 1, 1974.

7. " Evaluation Report on the Load Carrying Capacity of Chengdu Baihuatan Bridge," Report, Chongqing Jiaotong Institute , Dcember 1988. (in Chinese)

8. " Finte Element Analysis of Reinforced Concrete," State — of — the — Art — Report, ASCE, New York, 1982.

Damage Assessment and Remaining Life Prediction for Structures
Evaluation des dommages et de la vie restante des structures
Schadensbewertung- und Restlebensdauer-Prognose für Tragwerke

Lubin GAO
Assoc. Professor
Railway Eng. Res. Inst.
Beijing, China
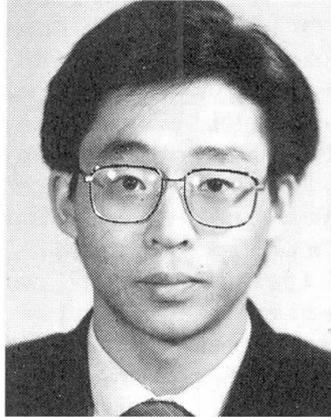
Lubin Gao, born 1965, member of IABSE, obtained Ph.D from CARS in 1989, M.S. from Tsinghua Univ. in 1986. At present he is majoring in structural engineering and engineering mechanics as well as computer applications.

SUMMARY
This paper firstly gives a brief review on the research of damage assessment and remaining life prediction for existing bridge structures in China. Secondly, a discussion on this topic is also presented. Finally a prototype expert system for damage assessment of railway bridges is introduced.

RÉSUMÉ
Après une introduction sur les recherches et l'évaluation des dommages et de la vie restante des structures de pont en Chine, et des commentaires sur les méthodes existantes, l'auteur propose un projet de système expert pour déterminer l'état des dommages et de la vie restante des structures de ponts ferroviaires.

ZUSAMMENFASSUNG
Der Beitrag gibt eingangs einen kurtzen Überblick über die chinesische Forschung bezüglich Schadensbewertung und Vorhersage der Restlebensdauer von Brückentragwerken. Nach einer Diskussion der Problematik wird der Prototyp eines Expertensystems für Schäden an Eisenbahnbrücken vorgestellt.

1. INTRODUCTION

The safety of railway transportation has been focused serious attention of railway administration, research and design branches, not only because railway accidents always induce heavy loss of the life and property of peoples, but also because the most important is it is directly related to traffic schedule of railway transportation. Of a lot of factors affecting railway traffic safety, it is the service state of railway track and railway structures which plays a significant role to. Firstly, railway construction, especially railway bridges have a long service life and difficult rehabilitation characteristics. Secondly repair expense of railway bridge is very great. Hence railway maintenance branches has a very important, long-time task which is bridge service state inspection. Since 1950's, damage assessment of railway bridges has been investigated and a lot of experimental data and experience have also been obtained. But due to the complexity of the problem, it is still a very important research project to start deepgoing investigation on damage assessment and remaining life prediction method for existing structures. At the end of the paper, a prototype expert system to diagnose damage state of railway bridges will be briefly introduced.

2. BRIEF REVIEW ON THE RESEARCH

For a long time, railway bridge inspectors and researchers in China have been searching for a reasonable and effective method to assess service state of railway bridges. But up till present, no well method has been developed, owing to the limit of experience and research work as well as the complexity of the problem. Existing approaches may be classified into two kinds: physical inspection and mechanical measurement, such as structural outward appearance observation for cracks and dynamic response test. Physical means for interior inspection include ultrasonic method etc. Not all of the existing methods is effective.

In Northern China, railway has served for a considerablly long time. Bridge damage is more serious. Hence Harbin Railway Administration Bureau has paid more attention to the research and practice of damage state inspection and assessment for bridges. Since 1979's, a lot of situ test data for dynamic response and time-domain properties of railway bridges have been accumulated, and a great deal of experience for diagnosing damage state of bridges has been obtained. They applied maximum transver dynamic displacement of bridge pier and some peculiarities of vibration wave of pier-head displacement as identifying rule to sum up into 10 types of damage for bridge pier.

China Academy of Railway Sciences started the investigation and research work on this topics in last 1970's. At the first stage of research, CARS has gathered a lot of situ dynamic test data

for existing bridges, which have been also analyzed, for example,
the effects of damage on frequencies, modes, time-domain and
frequency-domain peculiarity of bridges. Classifying the test
data of about 80 bridge piers, CARS has suggested a standard for
damage diagnosing of bridge pier.

The investigation on damage assessment for superstructure of
bridges in China started in middle 1980's. CARS firstly did a lot
of inspection work on riveted and welded steel bridges. Then a
great amount of tests on fracture mechanics and fatigue
properties of situ samples of bridge elements. For these kinds of
bridges, CARS has done about 10-year investigation and has
obtained some preliminary results. In recent years, CARS still
does an amount of researches on damage assessment method for
reinforced and prestressed concrete railway bridges, as well as
strengthening method for damaged bridge rehabilitation.

According to present research state, the investigation and
research on damage assessment and remaining life prediction
approaches for existing railway bridges must be continued.

3. PREPARE WORK IN DAMAGE ASSESSMENT PROCEDURE

Prepare work for damage assessment of existing structures is
composed of two stages:

* situ inspection and testing
* laboratory testing and analysis

The main objective in the first stage is to acquisite practical
structure geometric, physical and mechanical knowledge and
information about the bridge to be assessed. The methods to
inspect the bridge include outward appearance observation,
physical measurement for cracks etc. as well as mechanical test
to measure free vibration frequencies, modes and dynamic response
to loading etc.

3.1 Situ Inspection and Testing

Outward appearance observation

Outward appearnace observation for railway bridges is one of the
routine duties of bridge maintenance branches. From the
inspection, we can obtain basic knowledge and information about
bridge service state, such as

          cracks: length, location, direction, depth etc.
          crust of reinforcement: location, extent etc.
          deterioration of concrete: location extent etc.
          inclination of bridge pier: direction, degree etc.
          link of bridge and piers: state, relative displacement etc.

foundation: state

Interior defect inspection

On the basis of outward appearnace observation, interior defect inspection for existing bridges is mainly to survey interior damage of bridge structures by means of physical method, for example using ultrasonic approach to measure crack depth and interior cracks of structures.

Situ mechanical testing

The aim of situ mechanical testing is to acquisite basic mechanical properties of the bridge to be assessed, generally using dynamic testing to measure free vibration frequencies, modes and dynamic response to vehicle loading. In addition, situ testing work also include obtaining samples for laboratory test and some basic material property experiment such as concrete strength test etc.

3.2 Laboratory Testing and Analysis
_____

The main tasks in this stage composed of data treatment for the first stage, necessary laboratory test of situ samples in order to deliever sufficient information for damage assessment and remaining life prediction of the bridge assessed. Laboratory test is generally to measure fundamental properties, fracture mechanics and fatigue properties of samples of bridge structure and materials.

Time-domain and frequency-domain analysis as well as dynamic parameter identification are very useful to assess bridge service state. The second work in this stage is posttreating dynamic testing data recorded in situ test, including analysing and identifying physical and modal parameters, time-domain and frequency-domain peculiarities of the bridge.

4. DAMAGE ASSESSMENT AND REMAINING LIFE PREDICTION

From the prepare work, we have obtained some knowledge and information for geometric, physical and mechanical properties of bridge assessed. The remained work is to assess service state of the bridge and to predict its remaining life. How to do this work? The first problem is how to model and quantify damage.As discussed above, damage phenomena are very different and complex. So it is considerablly difficult modelling damage of structures.

As an example, we investigate effects of damage on dynamic properties of bridge pier in following so as to find some variables sensitive to damage.

(1) Frequencies of bridge pier
Dr. Sun [2] investigated frequencies of bridge pier with and
without cracks in 1991. The first four frequencies of a pier is
listed in Table 1, from which we may know the effect of damage on
frequencies of bridge pier.

Table 1. Frequencies of a bridge pier (Hz)

Mode	1	2	3	4
Normal pier	17.05	18.93	113.95	137.21
Cracked pier	16.39	17.42	110.51	-----

(2) Modal shape of bridge pier
Convex point may be found near cracks in modal shape of cracked
pier.

(3) Modal damping of bridge pier
Chen [3] found that modal damping of damaged bridge pier becomes
greater and greater as damage becomes larger.

(4) Maximum pier-head displacement
With the reduction of pier stiffness, maximum pier-head displace-
ment under vehicle loading becomes greater.

(5) Time-domain peculiarity
Forced vibration response wave is smooth, similar to harmonic
wave for good state bridge piers, but it may emerge some singular
peculiarities for damaged piers.

(6) Frequency-domain peculiarity
Power spectrum of damaged pier may be found with some differences
to that of normal pier, such as with a wider band and smaller
value at low frequency, a continuous spectrum and a greater
number of peaks etc.

For superstructure of railway bridge, the effect of damage is
more complex. In general, dynamic response parameters reflect the
synthesized properties of structures. Some local damages have no
evident effect on dynamic parameters. From identification of
system parameters, we can only obtain a global and average damage
description.

Here we classify damages of structures into two categories: local
damage and global damage. The first may also called nonstructural
damage, and the second structural damage. "Nonstructural" and
"structural" do not mean without or with effect on structural
capacity. But nonstructural damage only affects local stress and
deformation of strcutures, and does not greatly affect
macroscopic global displacement of structures. However the second
is directly reflected from global mechanical response, such as
frequencies, modes etc.

The first kind of damage includes local cracks, corrosion of reinforcement, exposure of concrete etc. The second is the worsening of structural materials.

4.1 Damage Tolerance Method

For the first kind of damage, we can use several characteristic variables to measure it. For example, using crack length l, crack depth a and crack open displacement d to describe a local crack in structures. In general,

Characteristic variables: { Ai / i=1,2,...n }

Assume the damage produce a response quantity J to local stress, deformation etc. of the structure:

Response quantity: J

Through fracture analysis and material test, we may obtain a critical value of J as Jc. A simple method to define local damage is

D=J/Jc
D=0   when J=0   undamaged structure
D=1   when J=Jc   local failure

This method for the first kind of damage is similar to the main idea of Damage Tolerance Method of fracture mechanics.

4.2 Combined Damage Theory-System Identification Method

According to damage theory, if there are cracks or vacancy in materials, elastic modulus of material will be reduced. The author [5] obtained:

$$\widetilde{E}=(I-D):E$$

where $\widetilde{E}$ and E are elastic tensors of damaged and undamaged materials respectively. D is called damage tensor. I is a unit tensor. In case of isotropy, it can be simplified as

$$\widetilde{E}=(1-D)E$$

where D is a damage scalar.

Applying system identification method, we can obtain elastic modulus distribution of damaged bridges. Therefore damage state of the bridges may be also identified.

The approach discussed above is called Combined Damage Theory-

System Identification Method.

4.3 Remaining Life Prediction

In order to predict remaining life of existing structures, it is necessary to model damage evoluting property of bridges. In general,

$$\dot{D}=f(D, t, F)$$
or
$$\delta D/\delta N=g(D, N, F)$$

where F represents external act. N represents loading cycles.

It is a very complex work to obtain the damage evoluting equation. Firstly we have to do deep investigation on damage mechanism. Secondly we must grasp a lot of experiment results for bridge materials and elements with and without typical damages.

If damage evoluting equation has been developed, remaining life of bridges assessed can be predicted from the present damage state and the future loading spectrum of the bridges.

$$Nr=Nf-Ns$$
$$D(N+dN)-D(N)=g(D(N), N, F)(N+dN-N)$$
$$D=Ds \quad \text{when } N=Ns$$
$$D=1 \quad \text{when } N=Nf$$

where Ds represents the present damage of the bridge.

5. A PROTOTYPE EXPERT SYSTEM FOR BRIDGE PIER ASSESSMENT

The expert system, DREPM-DP, is a prototype system developed by China Academy of Railway Sciences, which is based on an expert system tool DREPM. In acquisition of knowledges, domain knowledge and expert knowledge as well as an analyse module are used. The system has two kinds of knowledge representation method: frame representation and productive representation. A ask-answer blackboard is designed, which makes the system has a good human-machine interface.

DREPM-DP has been used to assess damage state of about 20 bridge piers. The diagnosing results are identical to practical situation.

Example: Haoshi River Bridge on Han-Dan Railline
The piers of the bridge is of a circular cross-section, enlargement foundation on rough sand with gravel layer. Bridge maintenance branch reported that Pier No.3 rocked greatly when train passed the bridge. In 1988, Zhengzhou Bridge Inspection Branch did situ vibration testing to the bridge. According to the

results recorded in the test, DREPM-DP gives such diagnosing results:

Pier No.2: little worse state, D=0.4
Pier No.3: very worse state, D=0.1
Pier No.4: worse state, D=0.25

6. CLOSE REMARKS

Damage state assessment and remaining life prediction for railway bridges are closely related to transportation safety. Deepgoing investigation on how to assess the state and to predict the life is very significant at present. According to the discussion above, it has been found following topics must be done futher studies:

(1) Modelling method for damage of bridges
(2) Damage criterion and damage-servicability relation
(3) Damage evoluting properties

REFERENCES

1. GAO Lubin, CHENG Qingguo, Fatigue and Life Prediction for High-speed Railway Bridges, IABSE Symposium, Leningrad, 1991

2. SUN Ning, Dynamic Behavior and Damage Diagnosing Expert System of Bridge Pier, Thesis for Doctorate Degree, China Academy of Railway Sciences, 1991

3. CHEN Xinzhong, Investigation on Dynamic Diagnosing Method for Bridge Pier Damage, Thesis for M.S. Degree, China Academy of Railway Sciences, 1986

4. GAO Lubin, CHENG Qingguo, Damage Assessment of Structures by Identification of Structure Dynamic Parameters, Proceedings of EASEC-3, Shanghai, 1991

5. GAO Lubin, A New Isotropic Damage Constitutive Model and Its Applications, China Railway Science Journal, Vol.10, No.2, 1989

Probabilistic Response of Reinforced and Prestressed Bridge Cross-Sections
Réponse probabiliste de sections de ponts en béton armé et précontraint
Wahrscheinliche Belastungsantwort von vorgespannten Stahlbetonbrückenquerschnitten

Juan R. CASAS
Dr. Eng.
Technical Univ. of Catalunya
Barcelona, Spain

Associate Professor. In 1988, he received his Ph.D. degree from UPC, where he took up his present appointment at the University. His major field of research concerns design, dynamic behaviour, experimental testing and reliability of bridges.

Juan A. SOBRINO
Civil Engineer
Technical Univ. of Catalunya
Barcelona, Spain
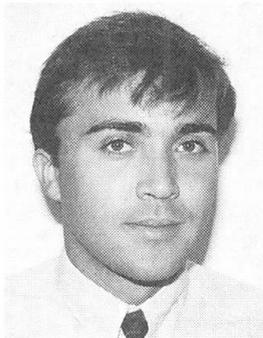
Research Assistant. He received his Ms. degree in 1990. He is working in research in load and resistance modeling for reliability analysis of existing bridges and structural evaluations. In 1991 he joined the concrete bridge group in the UPC.

SUMMARY

This paper is concerned with the recent available data obtained for modeling geometrical and material uncertainties for concrete bridges, and the use of these models to obtain the probabilistic response of reinforced and prestressed concrete bridge cross-sections. A parametric analysis is performed for explanning the basic features to evaluate the real response of existing bridges for reliability analysis and identifying the more relevant parameters for quality control or testing tasks.

RÉSUMÉ

L'article résume les données obtenues pour la modélisation de l'incertitude relative à la géométrie et les propriétés des matériaux employés dans la construction des ouvrages d'art en béton armé et précontraint, et leur utilisation pour la détermination de la réponse probabiliste de sections transversales de ponts. Une analyse paramétrique permet de mettre en évidence les principaux critères pour l'évaluation de la réponse réelle des ponts existants, d'analyser la fiabilité, et d'identifier les paramètres les plus importants à considérer dans le contrôle de qualité ou la rationalisation d'essais.

ZUSAMMENFASSUNG

Dieser Artikel beschreibt die neuesten verfügbaren Daten, die für die Modellierung von Geometrie- und Materialunsicherheiten bei Betonbrücken bestimmt wurden und die Verwendung dieser Modelle zur Bestimmung der wahrscheinlichen Belastungsantwort von vorgespannten Stahlbetonbrückenquerschnitten. Einer Parameterstudie wird durchgeführt, um die Hauptmerkmale der Bestimmung der wirklichen Belastungsantwort von existierenden Brücken sowie deren Zuverlässigkeitsanalyse zu erklären, ausserdem bestimmt sie die wichtigsten Parameter für die Qualitätskontrolle oder vorzunehmende Tests.

1.- INTRODUCTION

In order to obtain an accurate reliability analysis of existing or future structures it is necessary to use more realistic models for materials, geometrical variabilities and structural analysis, taking into account the non-linear behavior [1]. The use of analytical or semi-empirical relations for the obtention of the bridge section resistance available in design code must be improved.

The statistical parameters of geometrical variability and the uncertainties in the physical properties of the involved materials has been normally derived for the available literature data for building [2]. Nevertheless, in bridge construction both the construction considerations stipulated are different and more accurate techniques are used. Thus, a higher quality construction can be obtained. On the other hand, the available data are not directly suitable for other countries with different modes of construction or quality control. So that, more information should be obtained.

Recently, numerical methods to evaluate the structural cross-section response of prestressed and reinforced girders have been developed to obtain ultimate moment and shear responses and the moment-curvature relationship [3], and they has been widely used for bridge evaluation and code calibration [4]. There is a need for the analysis of other concrete bridge typical cross-sections.

2.- GEOMETRICAL VARIABILITY

The parameters involved in the geometrical shapes, alignment, configuration of building components are subjected to uncertainties due to different sources: form works, placement of reinforcing or prestressing steel, placing of concrete, assemblage procedures, etc. Geometrical variations affect both, the self weight of the structural elements, (dead load) and the cross section response (effective depth, concrete covers, etc.) Most of the different literature data available has been collected in Western Europe, USA and Japan, mainly for building structures [5] [6].

2.1.- Experimental data and proposed models

A large experimental data bank has been collected until now in different bridges recently built in Barcelona area (post-tensioned concrete slabs and one box girder bridge). Also, a large data has been obtained from a group of reinforced and prestressed concrete bridges (slabs and girder bridges) demolished, for urbanistic reasons because of the 1992 Olympic Games and the construction of new infrastructure, in Barcelona.

The parameters collected have been: Deck tickness in slab-girder bridges, geometric definition of girders, depth of slabs, thickness of top and bottom slabs in box girder bridge, effective depth of reinforcing, diameter of voids in voided slab, thickness of asphalt.

The measurements of all these variables have been analyzed in order to obtain the statistical parameters. A Kolmogorov-Smirnov test has been used to derive the theoretical probabilistic model. The probability distribution function included in these study were: Normal, Lognormal, Truncated Lognormal, Gamma and Truncated Gamma. For each of these distributions the Kolmogorov-Smirnov test provide a rational measurement of the approach. In many cases, all of these functions fitted well the sample, thus to simplify the rational use of the theoretical models the criteria was to select the Normal or Lognormal probability density distributions. The results are summarized in Table 1.

3.- MATERIAL UNCERTAINTIES

The available data and modeling for the physical uncertainties involved in the material and mechanical properties is very large [7] [8] [9]. Anywise, to obtain accurate models it is necessary to define the source and to process the samples that are homogeneous, in order to establish a suitable probability functions for a well definite random variable to use in further calculations.

In this paper, the data collected is restricted to materials recently used in concrete bridge construction in Spain, with a mean quality control of the materials and high quality control of construction.

Parameter X	Xnominal (mm)	Xmean X nominal	Xmin. Xmean	Xmax. Xmean	Standard Dev Xmean	Type of distribution
Deck Slab Girder Thick.	250.0	1.00	0.79	1.13	0.07	Normal
Horizontal dimensions of Girders	250 - 600	0.99-1.003	0.99	1.007	0.003 -0.007	Normal
Vertical dimensions of Girders	150 600	0.94 - 1.025	0.95	1.05	0.025 0.003	Normal
Depth of cast in situ Slabs	300 1800	0.996	0.94	1.05	0.026 0.015	Normal or Lognormal
Depth of top Reinforc.	266	1.006	0.91	1.07	0.045	Normal
Depth of bottom Reinf.	50	1.41	0.48	1.83	0.27	Normal
Thickness of top slab in Box Girder	250	0.95-1.03	0.89-0.92	1.06-1.10	0.02-0.07	Normal
Thickness of bottom slab in Box Girder	200 350-450	1.002 0.95-1.1	0.987 0.95-0.97	1.012 1.03-1.05	0.011 0.016-0.025	Normal
Diameter of voids (Slab)	1200-1400	0.97	0.98	1.02	0.007-0.008	Normal
Thickness of asphalt	45 - 80	0.95-1.14	0.58-0.76	1.25-1.53	0.26-0.11	Normal or Lognormal

The measurements of geometrical definition of girder cross- sections have been classified in vertical and horizontal dimensions.

Table 1.- Geometrical variability

3.1 - Concerning Concrete

Different samples of compressive strength of concrete have been processed to get the statistical parameters and to obtain a good fit. Normal and Lognormal PDF provide a rational approach for modeling this parameter. It is recommended to use Normal distribution for high quality concrete. The statistical data are summarized in Table 2, for three types of concrete.

Specified fc,k (MPa)	Age at test (days)	fc, mean (MPa)	fc,min / fc,mean	fc,max / fc,mean	C.O.V.	Type of distribution
25	7	22 - 30	0.71-0.85	1.13-1.19	0.08-0.11	Normal Lognormal
25	28	28 - 33	0.74-0.82	1.20	0.09-0.11	Normal Lognormal
30	7	34	0.81	1.19	0.14	Normal Lognormal
30	28	36	0.70	1.20	0.11	Normal Lognormal
35	7	30 - 35	0.72-0.88	1.09-1.16	0.07-0.11	Normal Lognormal
35	28	40 - 42	0.77-0.94	1.05-1.16	0.03-0.10	Normal Lognormal

Table 2 .- Compressive concrete strength

3.2 - Concerning prestressing steel

A large data bank has been processed for two different types of strands, 0.5" and 0.6", and steel 270K (186/167 MPa). The source has been the more important manufacturer of prestressing steel in Spain, which provided hundreds of quality control tests, conform to ASTM A-416 specifications. All these data corresponds to prestressing steel used in post-tensioning concrete bridges in the last 3 years. Analysis of data and results of the Kolmogorov-Smirnov test are summarized in Table 3. An example of the sample is shown in Figure 1.

Type of strand	Parameter X	X mean	X nominal	Xmin / Xmean	Xmax. / Xmean	C.O.V.	Type of distributi.
0.5 "	E modul.	197.0	190.0	0.96	1.04	0.018	Normal Lognormal
0.5 "	Ty, 0.2%	180.6	166.0	0.92	1.08	0.028	Normal Lognormal
0.5 "	T max	195.5	186.0	0.95	1.06	0.017	Normal Lognormal Gamma
0.6 "	E modul.	196.5	190.0	0.95	1.06	0.019	Normal Lognormal
0.6 "	Ty, 0.2%	247.0	238.0	0.94	1.08	0.022	Tr. Gamma Tr. Lognor
0.6 "	T max	271.6	266.0	0.96	1.07	0.018	Lognormal Normal

E = Deformation module (kN/mm2), Tmax = Tensile strength (kN) and Ty,0.2%= Yield force (kN).
Tr. Gamma= Truncated Gamma Tr. Lognorm= Truncated Lognormal.

Table 3 .- Prestressing Steel (270K) properties.

3.3 - Concerning reinforcing steel

The available data for reinforcing steel is not as large as in the case of prestressing. Different quality controls, made in some bridges, provide us the data. The mechanical properties are very related with the bar diameter in the analysis performed. The results are presented in Table 4 although its can not be significant until the data bank will be more representative.
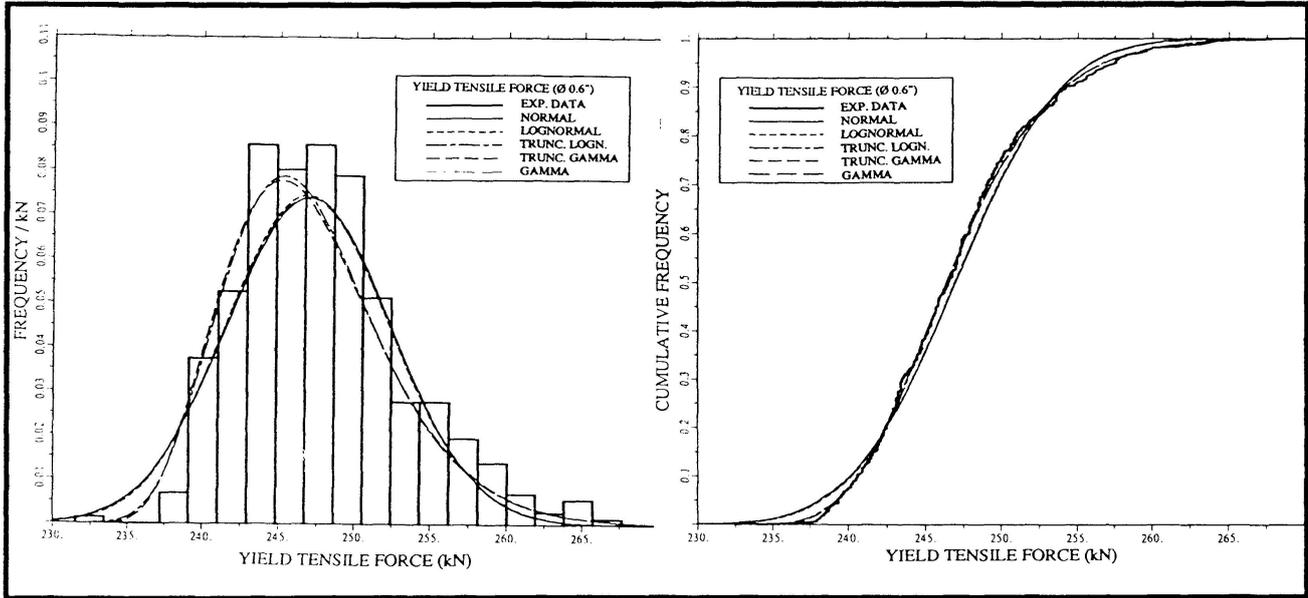

Figure 1.- Histogram, PDF and CDF curves, for yield tensile force prestressing steel. (strand 0.6")

Parameter X	X nominal	X mean	Xmin / Xmean	Xmax / Xmean	C.O.V.	Type of Distribution
Area,real / Area,nom	1.0000	1.003	0.98	1.05	0.002	Normal Lognormal
fy (kN/mm2)	51.0	58.0	0.91	1.10	0.057	Lognormal
f max (kN/mm2)	60.0	67.9	0.98	1.10	0.050	Lognormal

Table 4.- Reinforcing steel parameters (fy = yield tensile stress , f max= maximum tensile stress)

4.- RESISTANCE MODELS

Accurate resistance reliability models to obtain the real response of cross sections must take into account the real strain-stress relationship of the materials involved, and consider the uncertainty in the geometry and material properties [4].

A numerical procedure has been developed, considering the above mentioned needs, to obtain the moment, shear and torque response and the moment-curvature relationship of typical cross-sections

of reinforced and prestressed concrete bridges, conform to CEB Model Code [10]. The model has been computerized for easy application. In order to predict the probabilistic response and to fit a theoretical probability distribution a 400 Monte-Carlo simulations, for each case, were performed. The following assumptions were made:

- Strain-stress curves from CEB Model Code.

- The theoretical PDF used in the simulations are in conformity with data bank collected. The user can also use the experimental histogram.

- All parameters involved to define the cross-section geometry and strain-stress curves are considered as a independent random variable, in statistical sense.

- In each simulation all the above mentioned parameters are actualized.

Sensitivity analysis is made, in a recently built bridge in Barcelona (Fig. 2), to reveal the effects on the random response due to selected parameters such as:

- C.O.V of vertical and horizontal magnitudes of geometry, diameter of voids, fc, fct, yield stress of prestressing, effective steel prestress after losses, depth of prestressing.

The parametric analysis concerning C.O.V. is because of this statistic is directly correlated with quality of materials and construction and human error, for new bridges, or with the level of uncertainty in the unknown involved parameters of existing bridges. Thus, the more relevant parameters in the resistance evaluation can be selected and used to rationalize the test tasks and inspections.

4.1- Voided Slab. Margenat Bridge in Barcelona.

This is a simply supported prestressed concrete voided slab, cast in situ in 1991, with a span length of 27.40 m, the cross-section and the placement of prestressing are shown in Figure 2 [11]. The Moment-curvature relationships are shown in Figure 3, with design values (factored resistance) and with mean and characteristic values of parameters involved. Numerical results of the response value analyzed are given in Table 5. Due to the lack of space only the most relevant results of parametric study are summarized in Figures 4, 5, 6 and 7.
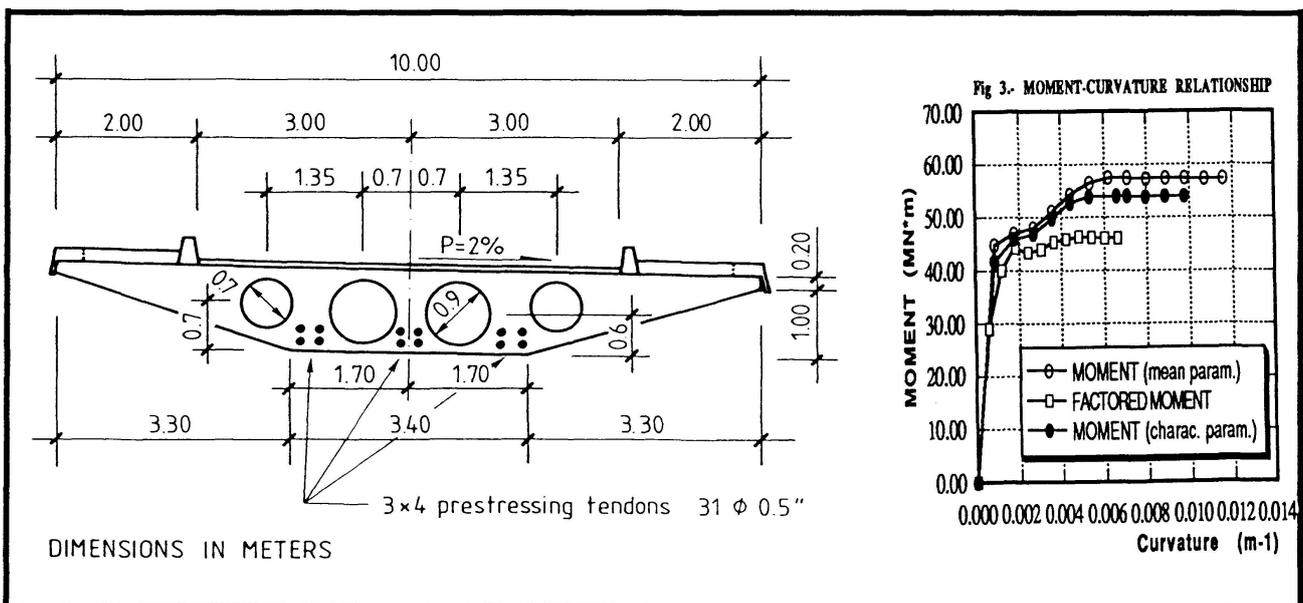

Figure 2.- Margenat bridge. Typical cross-section. Figure 3.- Moment-curvature relationship from decompression of concrete

Parameter X	$\frac{X \text{ mean}}{X \text{ nominal}}$	X mean	$\frac{X min}{X mean}$	$\frac{X max}{X mean}$	C.O.V.	Type of Distribution
Ultimate Bending-Moment (MN*m)	1. 254 * 1.067	57.45	0.92	1.10	0.034	Normal Lognormal
M, crack (MN*m)	1.00	32.48	0.90	1.14	0.046	Normal Lognormal Gamma
Inertia section (m4)	1.00	0.829	0.75	1.23	0.089	Lognormal Tr. Lognor. Gamma
Area section (m2)	1.00	6.657	0.91	1.08	0.032	Normal Lognormal

Table 5.- Simulation results. (* design value, factored resistance $\emptyset c = 1.5$ and $\emptyset s = 1.15$). Nominal values conform to CEB Model Code, with characteristic parameters.

The real case of cross-section herein studied yield a good example to evaluate the main important parameters involved in its ultimate resistance and serviceability behaviour. It is easy to realize that the most important parameters are related with geometry and not with those concerning with strength of material, due to the ductile behaviour. In the same way, the parametric study varying C.O.V of void diameters and with yield tensile stress of prestressing shows a not important correlation with the section properties analyzed.
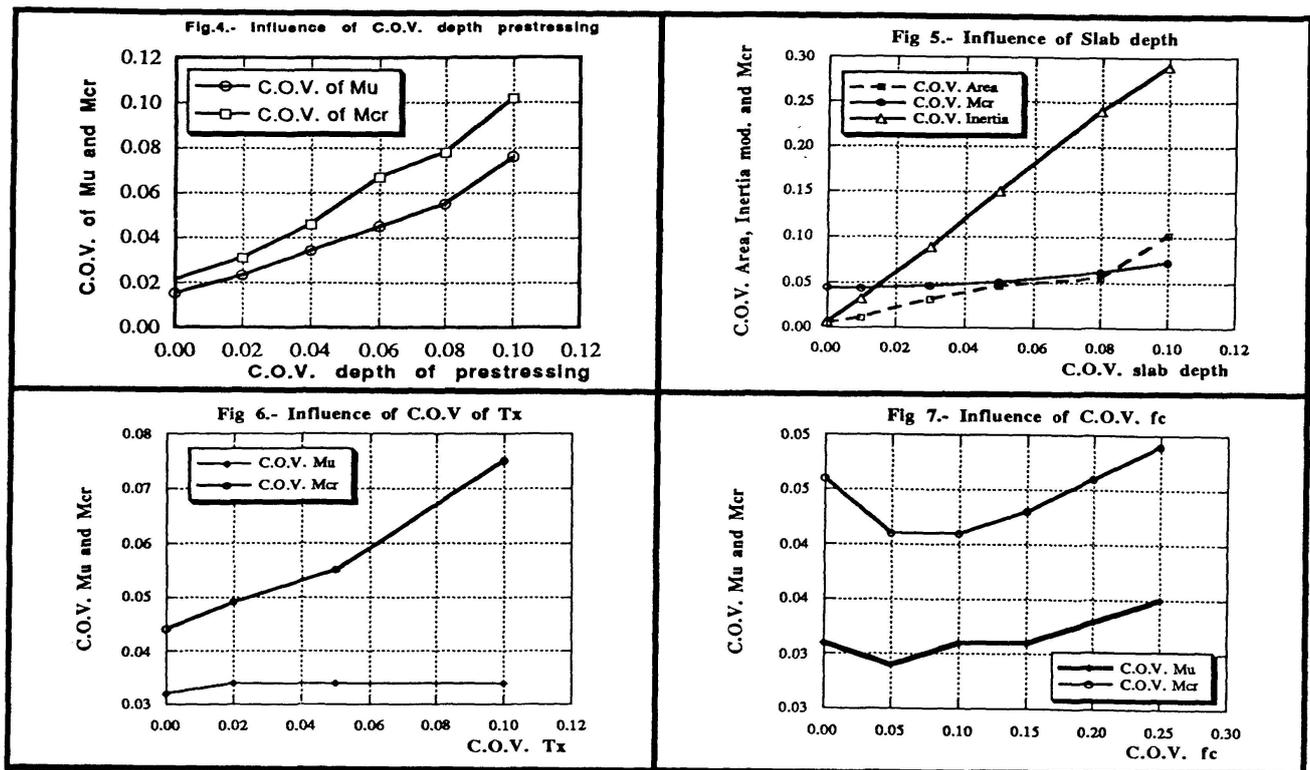
5.- CONCLUSIONS

5.1.- Conclusions concerning geometrical and material variability.

Due to the lack of data available for modeling geometrical and material variability in concrete bridges an important experimental data has been collected and presented. The statistical analysis of data fairly shows that different statistical parameters has to be considered in the analysis of reinforced and prestressed concrete bridges, which usually have a more accurate construction than buildings.

5.2. - Conclusions concerning probabilistic response of concrete bridges

The scarcity of analysis of the most typical cross-sections in concrete bridges has conducted to develop a numerical procedure to obtain the probabilistic response, in terms of moment, torque and shear, taking into account the non-linear behaviour of materials and the uncertainties in the parameters involved. A parametric study has been presented as a guideline to determine the sensitivity of resistance and geometrical properties of the cross-section to different varying C.O.V. of main parameters. The results show that the most important parameters to be correctly and accurately evaluated are cross-section geometry and depth of prestressing steel.

Fig.4.- Influence of C.O.V. depth prestressing

Fig 5.- Influence of Slab depth

Fig 6.- Influence of C.O.V of Tx

Fig 7.- Influence of C.O.V. fc

Note: Tx=prestress after losses, fc= compressive concrete strength.

7.- REFERENCES

1.- KARAGEORGOU, P. AND SKABARDONIS, A.; " Reliability of structural members under time-dependent loads" . Proceedings of the 4th specialty conference on Probabilistic and structural reliability, pp. 359-362, January, 1984.

2.-ELLINGWOOD, B. GALAMBOS, T.V., MAcGREGOR, J.G. AND CORNELL C.A.; "Development of a probability based load criterion for American national standard A58 ". National Bureau of Standards, NB's Special publication 577, Washintong, D.C., 1980.

3.-TING, S.C.;" The effects of corrosion on the reliability of concrete bridge girders"; Ph D Thesis, Department of Civil Engineering, University of Michigan, Ann-Arbor, Michigan, 1989.

4.-NOWAK, A.S.;" Calibration of LRFD bridge design code" NCHRP Project 12-33. Department of Civil Engineering, University of Michigan, Ann-Arbor, Michigan, 1992.

5.-CASCIATI, NEGRI AND RACKWITZ; " Geometrical variability in structural members and systems ". Joint Committee and Structural Safety. Working document, January 1991.

6.-MIRZA, S. A., MAcGREGOR, J. G.; " Variations in dimensions of reinforced concrete members". Journal of the Structural Division ASCE, Vol. 105, ST4, pp. 751-766, April, 1979.

7.-MIRZA, S. A., MAcGREGOR J.G. ; " Variability of mechanical properties of reinforcing bars ". Journal of the Structural Division ASCE, Vol. 104, ST4, pp. 921-937, May, 1979.

8.-MIRZA, S. A., HATZINIKOLAS, M., MAcGREGOR J.G. ; " Statistical description of strength of concrete". Journal of the Structural Division ASCE, Vol. 105, ST6, pp. 1021-1037, June, 1979.

9.-VEGH, L.;"Quality control and rehabilitation of concrete structures in Czechoslovaquia". Bull. of the International Assoc. for Shell and Spatial Structures, No 105, Vol. 32, pp. 41-49, April, 1991.

10.- CEB-FIP Model Code for concrete structures , Lausanne, 1990.

11.- CASAS J.R. and APARICIO A.C.; "Project of the bridge in Margenat street". Regional Government of Catalunya. 1991.

Dynamic Behaviour in Existing Concrete Bridges and Damage Detection
Comportement dynamique des ponts en béton et détection des dommages
Dynamisches Verhalten bestehender Betonbrücken zur Schadenerkennung

Ayaho MIYAMOTO
Prof. Dr.
Kobe Univ.
Kobe Japan

Hidenori MORIKAWA
Research Assoc.
Kobe Univ.
Kobe Japan

Yoshiaki KAJITANI
Dep. Dir.
Hyogo Prefecture Government
Kobe, Japan

A. Miyamoto, born 1949, received his Doctor of Engineering at Kyoto University in 1985. His recent research activities are in the areas of structural safety assessment on concrete bridges and establishment of design concept for concrete structures under impact loads.

H. Morikawa, born 1959, received his Master of Engineering degree from Kobe University in 1984. His current research activities are in structural safety and reliability analysis of concrete structures. He is now developing a fuzzy expert system for structural safety assessment of concrete bridges.

Y. Kajitani, born 1943, received his Master of Enginering degree from Kobe University in 1969. He is attached to the Road Construction Division and is now working on technical management related to middle span bridges, and also has great interest in integrated management system of steel and concrete bridges.

SUMMARY

In this paper, the sensivities of the dynamic behaviour of concrete bridges constituted by natural frequency, mode shape, damping and phase angle in damage detection is studied utilizing an analysis of the complex eigenproblem considering non-proportional damping and using dynamic loading tests on an existing bridge in which some specified artificial damage had been included. Also, a method of damage assessment for concrete bridges integrated from both the concise detection of damage location based on the difference in the sensitivities of modal parameters and the exact evaluation by localization and quantification of multiple damage based on the system identification method, is discussed.

RÉSUMÉ

Les sensibilités du comportement dynamique des ponts en béton constituées par la fréquence naturelle, la forme modale, l'amortissement et le déphasage sont examinées en vue de la détection des dommages, avec le recours à l'analyse de problèmes propres complexes, et en tenant compte de l'amortissement non proportionnel et des essais en charge dynamiques sur des ponts existants où quelques dommages artificiels spécifiques ont été induits. On y discute également une méthode d'estimation des dommages des ponts en béton intégrée à la fois par une détection concise de la localisation du dommage selon la différence des sensibilités des paramètres modaux et par une évaluation exacte par localisation et quantification des dommages multiples selon la méthode d'identification des systèmes.

ZUSAMMENFASSUNG

In dieser Arbeit wird die Empfindlichkeit im dynamischen Verhalten, ausgedrückt durch natürliche Frequenz, Modalform, Dämpfung und Phasenwinkel, von Betonbrücken in der Schadenserkennung untersucht. Dabei wird die Analyse von komplexen Eigenproblemen unter Berücksichtigung der nicht-proportionalen Dämpfung und dynamischer Belastungstests auf vorhandenen Brücken, bei denen spezifizierte künstliche Lasten aufgebracht wurden, eingesetzt. Ausserdem wird eine Methode der Schadensbewertung von Betonbrücken diskutiert, bei der die schnelle Erkennung der Schadenslage und die genaue Bewertung der Lage und Quantifizierung von mehrfachen integriert sind. Erstere basiert auf dem Unterschied der Empfindlichkeit modaler Parameter, während für letztere die Systemindenfikation eingesetzt wird.

1. INTRODUCTION

The need for damage assessment of existing concrete bridges by a combination of visual inspections, loading tests and analytical studies, has been pointed out with reference to the diagnosis of bridge serviceability [1]. Since there are a number of factors included in the relationship between the damage to existing bridges and dynamic behavior, it is necessary to develop an efficient method for damage detection based on dynamic loading tests [2]. The most important aspect of this problem is to focus on the dynamic sensitive parameters to the damage, because this has a significant influence on the accuracy of assessment.

In this paper, the sensitivities of dynamic behavior constituted by the natural frequency, the mode shape, the damping constant and the phase angle, for damage detection was studied using an analysis of the complex eigenproblem considering non-proportional damping and also dynamic loading tests. For the analytical study, the component mode synthesis (CMS) method, which is one type of coupling technique for substructures in the dynamic analysis was applied to the complex eigenproblem for simplification and an iterative analyses for damage detection was utilized. The system identification (SI) method was developed based on sequential linear programming (SLP), combined with the dynamic sensitivity analysis, to quantify the degree of damage for each member in the whole system.

For the application of this method to existing concrete bridges, parametric analyses for simply supported RC-T beam bridges in service were executed to evaluate the sensitivities of damage to dynamic behavior and to construct a concise flow for damage detection. Furthermore, the SI method was applied to the results from the dynamic loading tests, performed on an existing bridge in whichsome specified artificial damages were induced. Finally, the concise flow and the SI method were integrated, to enable an efficient damage assessment by multi-level and multi-aspect approaches.

2. ANALYTICAL METHOD FOR DAMAGE DETECTION OF EXISTING BRIDGES

2.1 Modeling of bridges

For existing concrete bridges, stiffness reduction of the main girder has been caused due to the interactive effect of flexural cracks and retrogression in the modulus of elasticity of the concrete, The safety of bridges is strongly influenced by this process as due to a change of load distribution and hence a reduction in load carrying capacity. In this research, the stiffness reduction and change of damping constant were considered to be the damage factors. The modeling of the target bridge was carried out by using a lumped mass gridform model of finite beam elements and spring elements for the elastic restraint of rotation at the supports. Fig.1 shows an example of the model for an existing RC-T beam bridge, "Nakaibashi" located in Hyogo prefecture in Japan.

2.2 Component mode synthesis method in the complex eigenproblem

The CMS method deals with the equation for the whole structure in modal coordinates obtained by synthesis of the boundary modes of substructures previously evaluated by modal analysis in the physical coordinates. When the whole structure is

(a) Analysis model

Girder A   Girder B   Girder C   (mm)

(b) Section of Nakaibahi bridge

Fig.1 Modeling of existing RC-T beam bridge

divided into n pieces of substructures, the equation of motion for the substructure i can be expressed by:

$$\begin{bmatrix} M_{aa}^i & M_{ab}^i \\ M_{ba}^i & M_{bb}^i \end{bmatrix} \begin{Bmatrix} \ddot{\delta}_{ia} \\ \ddot{\delta}_{ib} \end{Bmatrix} + \begin{bmatrix} C_{aa}^i & C_{ab}^i \\ C_{ba}^i & C_{bb}^i \end{bmatrix} \begin{Bmatrix} \dot{\delta}_{ia} \\ \dot{\delta}_{ib} \end{Bmatrix} + \begin{bmatrix} K_{aa}^i & K_{ab}^i \\ K_{ba}^i & K_{bb}^i \end{bmatrix} \begin{Bmatrix} \delta_{ia} \\ \delta_{ib} \end{Bmatrix} = \begin{Bmatrix} 0 \\ f \end{Bmatrix} \tag{1}$$

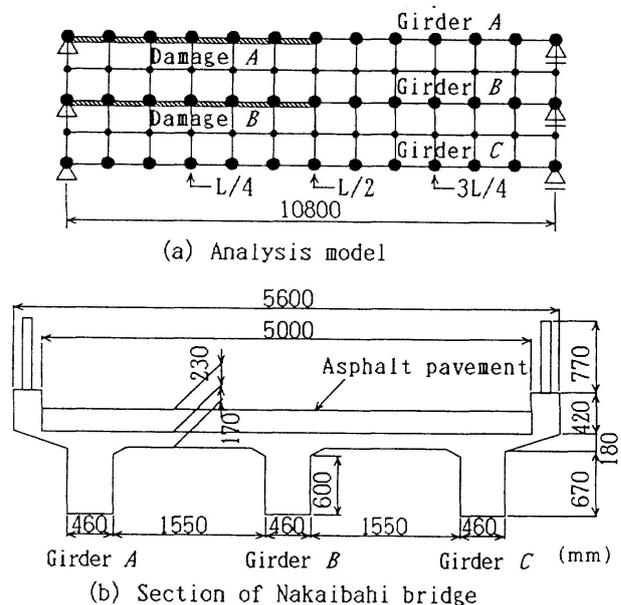where subscript a, b denote the internal area and the boundary area, respectively.

By using Guyan reduction of the stiffness matrix, a correlation between the displacement in the internal area and the boundary area can be expressed by:

$$\delta_{ia} = -\left[K^i_{aa}\right]^{-1}\left[K^i_{ab}\right]\delta_{ib} = T_i\,\delta_{ib} \qquad (2)$$

After this, an analysis of the complex eigenproblem for the synthesized whole structure, of which the matrix size is reduced to the degree of freedom for the boundary area of each substructure, is carried out. Displacement at the boundary area b can be evaluated in the form of complex conjugates by linear combination of each mode as:

$$y_b = \phi_b\,\xi_b \qquad (3),$$

where $\phi_b = \left[\phi_{b1},\ \overline{\phi}_{b1},\ \phi_{b2},\ \overline{\phi}_{b2},\ \cdots,\ \phi_{bk},\ \overline{\phi}_{bk}\right]$: the complex mode matrix,

k denotes the adopted number of modes, $y_b = \left\{\dot{\delta}_b,\ \delta_b\right\}^T$, $\xi_a = \left\{\xi_{1b},\ \xi_{2b},\ \cdots,\ \xi_{nb}\right\}^T$: the modal coordinates.

On the other hand, carrying out the analysis of the constrained mode for each substructure, displacement at the internal area a for each substructure can be expressed by:

$$y_{ia} = \left[T_i\phi_{ib},\ \phi_{ia}\right]\xi_i \qquad (4),$$

where $\phi_{ia} = \left[\phi_{ia1},\ \overline{\phi}_{ia1},\ \phi_{ia2},\ \overline{\phi}_{ia2},\ \cdots,\ \phi_{iam},\ \overline{\phi}_{iam}\right]$: the complex mode matrix,

m denotes the adopted number of modes, $\xi_i = \left\{\xi_{ib},\ \xi_{ia}\right\}^T$, $T_i = \begin{bmatrix} T_i & 0 \\ 0 & T_i \end{bmatrix}$

Displacement of the whole structure can be expressed by using the modes at the boundary area and the internal area, as:

$$\{y_b,\ y_a\}^T = X\ \{\xi_b,\ \xi_a\}^T = X\ \xi \qquad (5),$$

where $y_a = \{y_{1a},\ y_{2a},\ \cdots,\ y_{na}\}^T$, $\xi_a = \{\xi_{1a},\ \xi_{2a},\ \cdots,\ \xi_{na}\}^T$,

$$X = \begin{bmatrix} \phi_b & 0 \\ T\phi_b & \phi_a \end{bmatrix},\quad T = \begin{bmatrix} T'_1 & & & \mathbf{O} \\ & T'_2 & & \\ & & \ddots & \\ \mathbf{O} & & & T'_n \end{bmatrix},\quad \phi_a = \begin{bmatrix} \phi'_{1a} & & & \mathbf{O} \\ & \phi'_{2a} & & \\ & & \ddots & \\ \mathbf{O} & & & \phi'_{na} \end{bmatrix}$$

Finally, the equation of motion for the whole structure can be written as:

$$X^T P X\ \ddot{\xi} + X^T Q X\ \xi = 0 \qquad (6),$$

where $P = \begin{bmatrix} 0 & M_{bb} & 0 & M_{ba} \\ 0 & M_{ab} & 0 & M_{aa} \\ M_{bb} & C_{bb} & M_{ba} & C_{ba} \\ M_{ab} & C_{ab} & M_{aa} & C_{aa} \end{bmatrix}$, $Q = \begin{bmatrix} -M_{bb} & 0 & -M_{ba} & 0 \\ -M_{ab} & 0 & -M_{aa} & 0 \\ 0 & K_{bb} & 0 & K_{ba} \\ 0 & K_{ab} & 0 & K_{aa} \end{bmatrix}$

By analyzing the eigenproblem for Eq.(6), the modal parameters for the whole structure can be obtained. Furthermore, substituting the modes evaluated by Eq.(6) into Eq.(5), the modes of the whole structure in the physical coordinates can be obtained. The degree of freedom for this analysis is the sum of the adopted number of modes for the whole structure synthesized by the modes for the boundary area of all substructures; $2k$, and the adopted number of modes for the internal area of all substructures; $2\Sigma m_i$, ($i=1$, n, n: number of substructures), and it can be seen to be much less than the total degree of freedom for the whole structure. Through study of the accuracy of this method using the existing bridge model shown as Fig.1, it was founded that the results of this analysis were sufficiently accurate for the target modes of bridge vibration as shown in Fig.2, even if the adopted degree of freedom for the whole structure was half the total degree of freedom.
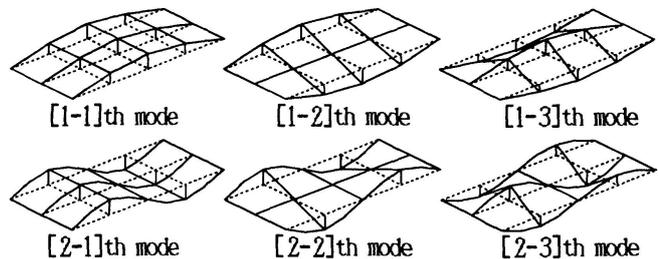

[1-1]th mode [1-2]th mode [1-3]th mode

[2-1]th mode [2-2]th mode [2-3]th mode

Fig.2 Shape of target modes

2.3 SI method using sensitivity analysis

The SI method [3] is one type of back analysis method, which can be used to identify system parameters such as the flexural rigidity corresponding to the degree of damage in the problem, by minimizing the error between the mechanical behavior as obtained from test and analysis. Here, the existing concrete bridge was modeled as shown in Fig.1, considering spring elements for the friction

restraint of rotation at the supports. In this research, the sensitivity analysis of damage to mechanical behaviors and the SLP method were integrated. The objective function was defined as minimizing the total squared error between the mechanical behavior obtained from the field test and the analysis, by:

$$F = W_1 \left(\frac{\mu_p}{\mu_p^m} - 1 \right)^2 + W_2 \sum_{k=1}^{n} \left(\frac{Z_{pk}}{Z_{pk}^m} - 1 \right)^2 \rightarrow min \quad (7)$$

where p is the order of normal vibration, n is the number of measuring points, μ, μ^m are the eigenvalues obtained from the analysis and the field test, respectively, Z, Z^m are the normalized modes of vibration, and W_1, W_2 are the weights for the eigenvalue and the vibration modes. Here, it is assumed that $W_1=1.0$, $W_2=1/n$.

The sensitivity (derivative) of the design variable(for identification, here assign it the rigidity K_i, $i=1\sim l$, l: the number of members) to the objective function, can be expressed by:

$$\frac{\partial F}{\partial K_i} = \frac{2W_1}{\mu_p^m} \left(\frac{\mu_p}{\mu_p^m} - 1 \right) \frac{\partial \mu_j}{\partial k_i} + \sum_{k=1}^{n} \frac{2W_2}{Z_{pk}^m} \left(\frac{Z_{pk}}{Z_{pk}^m} - 1 \right) \frac{\partial Z_j}{\partial k_i} \quad (8)$$

where

$$\frac{\partial \mu_p}{\partial k_i} = Z_p^T \frac{\partial K}{\partial k_i} Z_p , \quad \frac{\partial Z_p}{\partial k_i} = \sum_{j=1}^{n} \left(- \frac{1}{\mu_j^m - \mu_p^m} Z_j^T \frac{\partial K}{\partial k_i} Z_p \right) Z_j$$

and K is the stiffness matrix of the whole structure.

Following this, identification of the design variables can be performed by applying the SLP method using the objective function and its derivative for the design variables. Fig.3 shows the flow of the SLP method for the dynamic problem. Firstly, the initial values of the design variables are evaluated by analysis. Linearization of the objective function is then carried out within the region of movement limits for the design variables, and a search for the minimum point of the objective value is tried using the simplex method. In the event that the change of design variables exceeds the movement limits, reanalysis of the modal parameters and restart of the search for the minimum values from updated initial values are executed by the same procedure iteratively up to the stage at which the objective function is within the allowable limits.

3. APPLICATION TO AN EXISTING RC BRIDGE WITH ARTIFICIAL DAMAGE

3.1 Outline of target bridge

The target existing bridge "Oyasubashi" is 27 years old and a simply supported 4 girder RC-T beam bridge with a skew angle of 46 degrees and a span length of 14.7m. This bridge seemed to be almost intact according to the results of visual inspections. Fig.4 shows an outline section for this bridge.

3.2 Inducement of artificial damage

The artificial damage corresponding to
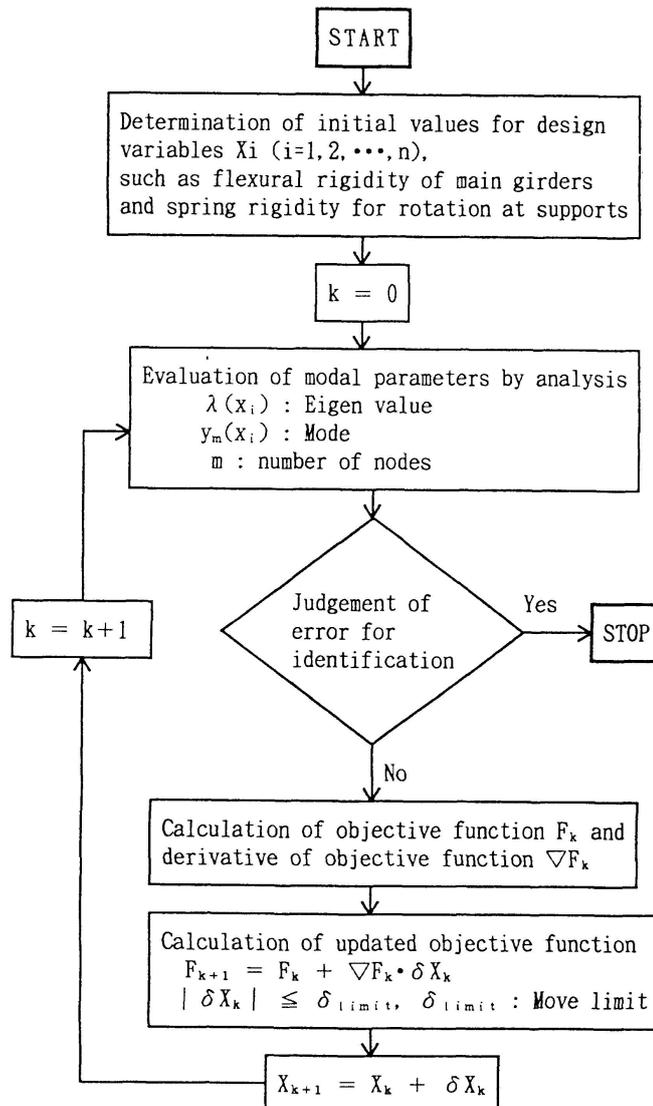

Fig.3 Flow of SLP (for dynamic problem)

flexural cracks in concrete in the tensile region were induced partially in the girders A and B as shown in Fig.5. Introduction of cracks was carried out by core boring along a vertical line from the bottom surface of concrete in the tensile region to the neutral axis, as shown in Fig.6. The core concrete blocks were then replaced in the holes from which they had been extracted, in order to avoid altering the weight of the girders.

3.3 Procedure for field test [4]

Prior to the field test, the target bridge was modeled as the lumped mass system shown in Fig.7, and the modal parameters were evaluated by analysis. From this a measurement method was determined focusing the antinodes of target vibration modes, as shown in Fig.5. Positions of forced vibrations by falling mass were arranged to obtain the various modes of vibration and the mass dropping was carried out from about 70cm height for ten times at the same loading point to cancel white noise and to obtain a stable average value. The modal analysis [5] was then applied to the acceleration data to identify the modal parameters.

3.4 Identification of damage parameters

The stiffness reduction of main girders was identified by the SI method based on the [1-1]th eigenvalue and eigenvector obtained from the field tests, using the following procedure:

(1)For the target bridge before inducement of the artificial damage, the system parameters constituted by the stiffness of main girders and cross beam, and the spring coefficient of rotation at the supports, were identified.

(2)After inducement of the artificial damage, the stiffness of the main girder in the damaged region and the spring coefficient of rotation at supports were identified under the condition that the girder stiffness except for damaged region was fixed at the value identified in (1).

Table.3 shows the results of the above procedure. According to the results, the change of natural frequency due to inducement of artificial damage is about 8% i.e. relatively great. The results of the SI method can be seen to show that the spring rigidity of rotation at the supports changed sharply due to

Fig.4 Section of *Oyasubashi* bridge

FIg.5 Outline of dynamic loading test
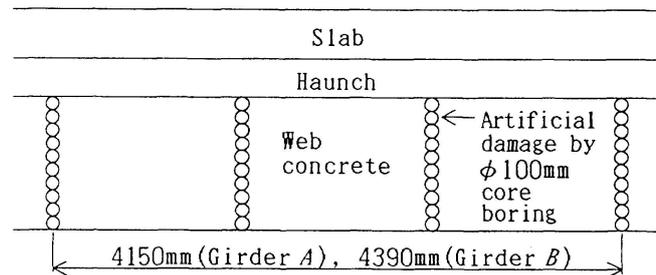
Fig.6 Inducement of artificial damage
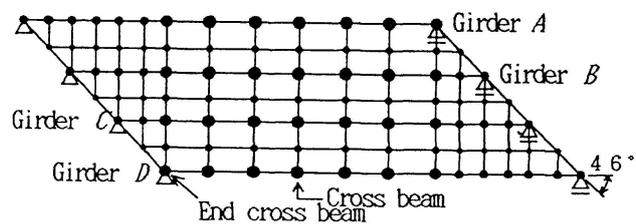
Fig.7 Analysis model for *Oyasubashi* bridge

inducement of the damage, although this bridge has simple support conditions in its design. In such cases, the SI method considering the spring rigidity of rotation at the supports as the design variables is effective. Identified girder stiffness before inducement of the damages was equivalent to the theoretical value considering the stiffness of concrete in the tensile region, and it agreed with the results of visual inspections and material tests of concrete cores extracted from the target bridge. Also the evaluated degree of damage was then relatively great and qualitatively matched the theory.
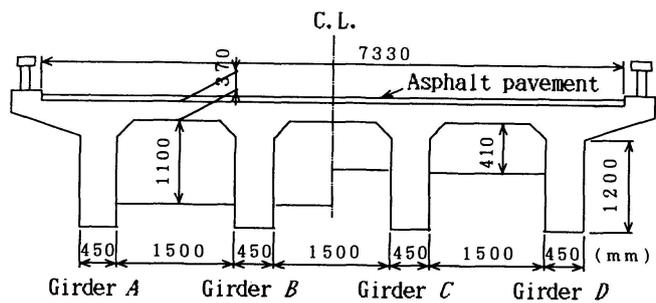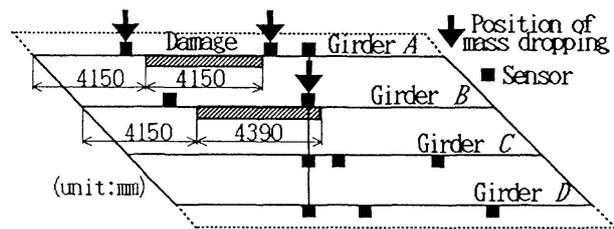
Table 1 Results of damage detection for *Oyasubashi* bridge

	Girder stiffness(×10¹²Kg·cm²) Girder				Spring rigidity of rotation at supports (×10⁹kg·cm/rad) Girder								1st natural frequency (HZ)
	A	B	C	D	A		B		C		D		
Theoretical value	7.198	6.755	6.755	7.255	—		—		—		—		—
Identified value without damage	8.242	7.701	7.160	6.346	1.310	1.310	1.100	1.100	0.900	0.900	0.690	0.690	12.69
Identified value with damage	5.496*	5.671*			0.0203	0.0122	0.0100	0.0089	0.0075	0.0073	0.0046	0.0044	11.71

* : Value at damaged region

4. EFFECTIVENESS OF MODAL PARAMETERS IN DAMAGE DETECTION

4.1 Modeling of bridge with damage

The target bridge is shown in Fig.1, and this was modeled considering partial damage. For the damage condition, the change of damping constant in the region of 0~30% in the region of A, B were assumed.
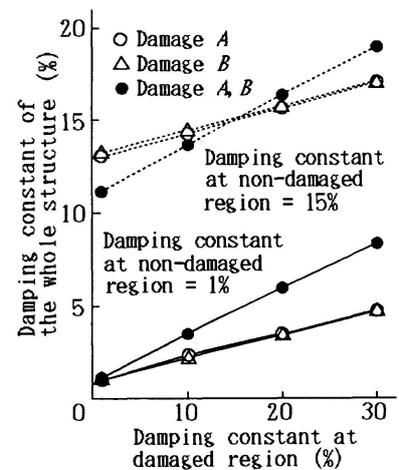
4.2 Damping characteristics

Fig.8 shows the relationship between the change of damping constant in the damaged area and that for the whole bridge system. For the [1-1]th mode of vibration, the sensitivities of damage A and B are the same and have linearity, independently of the change of damping constant in the non-damaged area. On the other hand, according to the results for the [1-2]th mode, damage B in girder B which is the node of vibration has no influence on the whole bridge system. Accordingly, localization of the damage can be carried out using the damping characteristics for both the [1-1]th and [1-2]th modes.
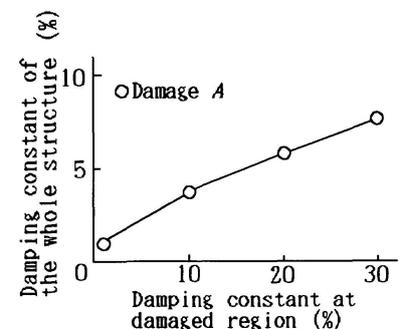
4.3 Phase angle

Fig.9 a)~c) shows the relationship between the change of damping constant in the damaged area and the difference in phase angle for each girder for the [1-1]th mode of vibration. Here, the difference in phase angle was evaluated on the basis of the phase angle at the midpoint of girder B. The difference in phase angle in the damaged girder is greatest, in particular, the influence of damage A is significant. The sensitivities of these parameters have linearity independently of the change of damping constant in the non-damaged area. On the other hand, Fig.9 d) shows the result for the [2-1]th mode and it can be seen that the sensitivity of damage A is great and the difference in phase angle between girder A and C is about 0.5rad i.e. largest. Accordingly, localization of the damage can be carried out by using these characteristics, similar to the above-mentioned damping characteristics.

4.4 Flow of damage detection based on modal parameters

Fig.10 shows the flow of damage detection by localization and quantification based on the sensitivities of modal parameters to damages. Firstly, a brief evaluation for the location of damage can be carried out using all or a portion of modal parameters constituted by natural frequencies f_{1-1}, f_{1-2}, f_{2-2}, damping constants ζ_{1-1}, ζ_{1-2}, and phase differences ψ_{1-1}, ψ_{2-1}. At the first

Fig.8 Damping characteristics

(a) [1-1]th mode with damage A, Damping constant at non-damaged region = 1%

(b) [1-1]th mode with damage A, Damping constant at non-damaged region = 15%

● ● L/4 of GirderA
■ ■ L/2 of GirderA
▲ ▲ 3L/4 of GirderA
○ ○ L/4 of GirderB
△ △ 3L/4 of GirderB
● ● L/4 of GirderC
■ ■ L/2 of GirderC
▲ ▲ 3L/4 of GirderC

(c) [1-1]th mode with damage B

● ● L/4 of GirderA
■ ■ L/2 of GirderA
▲ ▲ 3L/4 of GirderA
○ ○ L/4 of GirderB
△ △ 3L/4 of GirderB
● ● L/4 of GirderC
■ ■ L/2 of GirderC
▲ ▲ 3L/4 of GirderC

● ● L/4 of GirderA
▲ ▲ 3L/4 of GirderA
● ● L/4 of GirderC
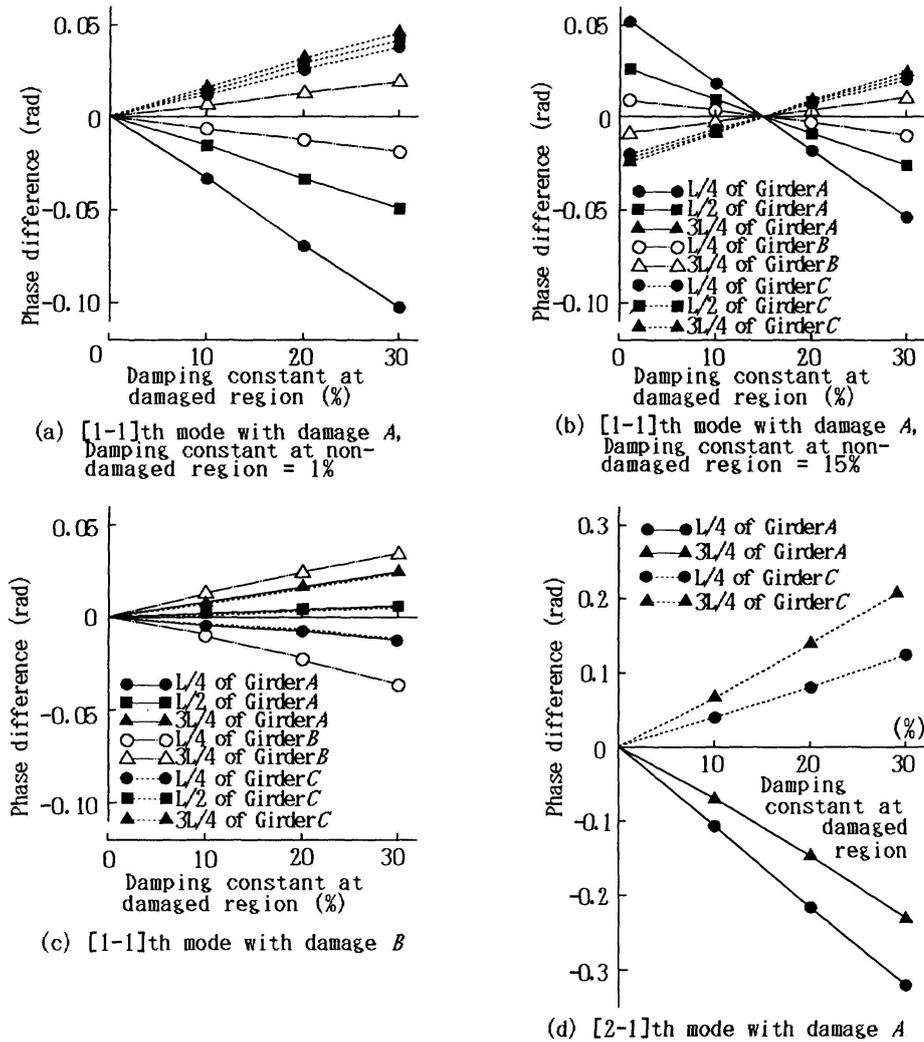▲ ▲ 3L/4 of GirderC

(d) [2-1]th mode with damage A

Fig.9 Characteristics of phase angle

step, the existence of damage can be detected by searching whether the parameters $(f_{1-1}$ and $f_{2-1})$, ζ_{1-1}, ψ_{1-1} indicate large values. After this, at the second step, localization of the damages i.e. the distinction between damage the inside girder or the outside girder, can be carried out by searching whether parameters f_{2-2}, ζ_{1-2}, ψ_{2-1} indicate large values. Though the above evaluation can be carried out independently for each modal parameter, the final decision for damage detection should be carried out comprehensively by comparison among the results from all parameters. Furthermore, the exact evaluation by localization and quantification of multiple damages can be carried out by the SI method. As the above mentioned procedure, the concise flow and the SI method can be integrated, to enable an efficient damage assessment by the multi-level and multi-aspect approaches.

5. CONCLUSIONS

The main conclusions obtained from this study can be summarized as follows:

(1) For the simplification of analysis of the complex eigenproblem considering non-proportional damping, the CMS method was applied and its suitability was demonstrated.

(2) The SI method based on dynamic sensitivity analysis and the SLP method has been studied and applied to the results of dynamic loading tests performed on an existing concrete bridge in which some specified artificial damage was induced.

(3) The sensitivities of dynamic behaviors to damage were evaluated by analysis and the results could be seen to show that the [2-1]th and [2-2]th natural frequencies, the [1-1]th, [1-2]th and [2-1]th damping constants, and the [1-1]th and [2-1]th phase differences had high sensitivity.
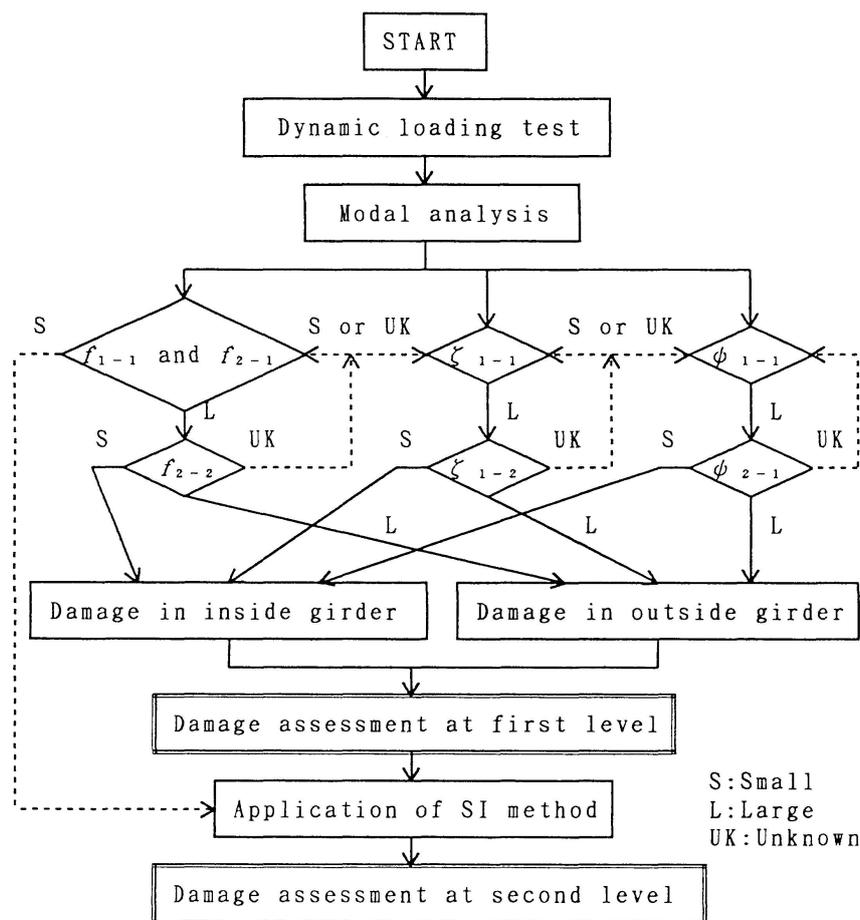
Fig.10 Flow of damage detection

(4)By using these modal parameters, a concise flow of the damage detection without any complex analysis was constructed. Furthermore, this concise flow and the SI method were integrated, to allow efficient damage assessment by multi-level and multi-aspect approaches.

REFERENCES

1. Natke, H. G. and Yao, J. T. P. (ed.), Structural Safety Evaluation Based on System Identification approaches, Proceedings of the Workshop at Lambrecht/Pfalz, Friedr. Vieweg & Sohn, 1988.
2. Nowak, A. S. (ed.), Bridge Evaluation, Repair and Rehabilitation, Proceedings of the NATO Advanced Research Workshop on Bridge Evaluation, Repair and Rehabilitation, 1990.
3. Douglas, B. M. and Reid, W. H., Dynamic Tests and System Identification of Bridges, Proceedings of ASCE, Vol.108, No.ST10, 1982.
4. Morikawa, H. and Miyamoto, A., Structural Safety Evaluation and Remaining Life Prediction of Existing Concrete Bridges, Proceedings of the 17th Conference on Our World in Concrete & Structures, 1992.
5. Ewins, D. J., Modal Testing-Theory and Practice, Research Studies Press, 1984.